

Cardiac-Specific Overexpression of Human Stem Cell Factor Promotes Epicardial Activation and Arteriogenesis After Myocardial Infarction

Fu-Li Xiang, MD, PhD; Yin Liu, PhD; Xiangru Lu, MD; Douglas L. Jones, PhD; Qingping Feng, MD, PhD

Background—The adult epicardium is a potential source of cardiac progenitors after myocardial infarction (MI). We tested the hypothesis that cardiomyocyte-specific overexpression of membrane-associated human stem cell factor (hSCF) enhances epicardial activation, epicardium-derived cells (EPDCs) production, and myocardial arteriogenesis post MI.

Methods and Results—Wild-type and the inducible cardiac-specific hSCF transgenic (hSCF/tetracycline transactivator) mice were subjected to MI. Wilms tumor-1 (Wt1)-positive epicardial cells were higher in hSCF/tetracycline transactivator compared with wild-type mice 3 days post MI. Arteriole density was significantly higher in the peri-infarct area of hSCF/tetracycline transactivator mice compared with wild-type mice 5 days post MI. In cultured EPDCs, adenoviral hSCF treatment significantly increased cell proliferation and growth factor expression. Furthermore, adenoviral hSCF treatment in wild-type cardiomyocytes significantly increased EPDC migration. These effects of hSCF overexpression on EPDC proliferation and growth factor expression were all abrogated by ACK2, a neutralizing antibody against *c-kit*. Finally, lineage tracing using ROSA^{mTmG};Wt1^{CreER} mice showed that adenoviral hSCF treatment increased Wt1⁺ lineage-derived EPDC migration into the infarcted myocardium 5 days post MI, which was inhibited by ACK2.

Conclusions—Cardiomyocyte-specific overexpression of hSCF promotes epicardial activation and myocardial arteriogenesis post MI. (*Circ Heart Fail.* 2014;7:831-842.)

Key Words: heart failure ■ myocardial infarction ■ stem cell factor ■ stem cells ■ regeneration

Cardiovascular disease remains a leading cause of death worldwide.¹ In the past decade, adult stem cell therapy has emerged as a promising new strategy for ischemic heart disease.² To this end, both cardiac and extracardiac progenitor cells have been demonstrated to improve cardiac function after myocardial infarction (MI).² The epicardium-derived cells (EPDCs) are cardiac progenitors that contribute to coronary artery formation during embryonic heart development.³⁻⁵ Transplantation of adult EPDCs into the ischemic myocardium in mice preserves cardiac function and attenuates ventricular remodeling via enhancement of neovascularization, suggesting their therapeutic potential in cardiac repair post MI.⁶

Clinical Perspective on p 842

During early heart morphogenesis, cells from the proepicardial organ migrate to the looping heart tube to form the epicardium.⁷ A fraction of these cells undergoes epithelial to mesenchymal transition (EMT), invades into the myocardium and becomes EPDCs, which give rise to smooth muscle cells, perivascular, and interstitial fibroblasts, and forms coronary

arteries with contributions from the endocardium and sinus venosus.⁸⁻¹¹ Wilms tumor-1 (Wt1) is expressed in the EPDCs and promotes EMT,¹² whereas its expression is turned off in fully differentiated EPDCs.¹³⁻¹⁵ The adult epicardium is inactive under normal physiological conditions, but can be reactivated and produces EPDCs after MI. Some of the EPDCs also express *c-kit*.^{16,17} However, the number of endogenously generated EPDCs is not sufficient for adequate cardiac repair post MI. Measures that promote epicardial activation and EPDC production may enhance cardiac repair post MI.

Stem cell factor (SCF) binds to *c-kit* and promotes survival, proliferation, mobilization, and adhesion of all *c-kit*-expressing cells.¹⁸ Alternative splicing leads to 2 isoforms of SCF, the soluble and the membrane-associated isoforms, which differ in the absence or presence of a proteolytic cleavage site encoded by exon 6.¹⁹ The membrane-associated SCF is the dominant isoform in vivo and induces more persistent and long-term support of target cell survival. We have shown that cardiac-specific overexpression of membrane-associated human SCF (hSCF) improves animal survival and cardiac

Received August 6, 2013; accepted August 7, 2014.

From the Departments of Physiology and Pharmacology (F.-L.X., Y.L., X.L., D.L.J., Q.F.) and Medicine (D.L.J., Q.F.), and Lawson Health Research Institute (D.L.J., Q.F.), Western University, London, Ontario, Canada.

The Data Supplement is available at <http://circheartfailure.ahajournals.org/lookup/suppl/doi:10.1161/CIRCHEARTFAILURE.114.001423/-/DCI>.

Correspondence to Qingping Feng, MD, PhD, Department of Physiology and Pharmacology, Western University, London, Ontario, Canada N6A 5C1. E-mail qfeng@uwo.ca

© 2014 American Heart Association, Inc.

Circ Heart Fail is available at <http://circheartfailure.ahajournals.org>

DOI: 10.1161/CIRCHEARTFAILURE.114.001423

function post MI.²⁰ However, the underlying cellular mechanisms require further investigation. In the present study, we hypothesized that inducible cardiomyocyte-specific overexpression of hSCF promotes epicardial activation and EPDC production post MI. To test this hypothesis, mice with cardiomyocyte-specific overexpression of hSCF were subjected to coronary artery ligation to induce MI. Epicardial Wt1 expression, myocardial growth factor levels, and arteriole density were studied. Furthermore, cell fate of Wt1 expressing epicardial cells post MI was determined using lineage tracing. Our results demonstrated that cardiomyocyte-specific overexpression of hSCF enhances epicardial activation and arteriogenesis post MI.

Methods

Experimental Animals

Animals in this study were handled in accordance with the Guide for the Care and Use of Laboratory Animals published by the US National Institute of Health (NIH publication No. 85-23, revised 1996). The conditional cardiac-specific overexpression of hSCF and tetracycline transactivator (tTA) double-transgenic (hSCF/tTA) mice were generated as described previously.²⁰ The hSCF was expressed on the sarcolemma of cardiomyocytes in hSCF-tTA mice (Figure IA in the Data Supplement). Furthermore, soluble hSCF was not detectable in the serum of hSCF/tTA mice (Figure IB in the Data Supplement). In the doxycycline group, mice were treated with doxycycline (0.2 mg/mL in drinking water) to turn off hSCF overexpression starting from 2 weeks before the surgeries. The membrane-tomato/membrane-green (mTmG)-targeted Rosa26 mice (stock No. 7576) and Wt1^{CreER} mice (Stock No. 010912) were purchased from Jackson Laboratory and bred to generate ROSA^{mTmG};Wt1^{CreER} mice. These reporter mice were treated with tamoxifen (40 mg/kg, IP) for 5 days before surgery to trace the lineage of Wt1⁺ cells in the myocardium post MI. To inhibit *c-kit* function, mice were injected intraperitoneally with 100 μ g *c-kit*-neutralizing antibody ACK2 (a gift from Dr Shin-Ichi Nishikawa, Kyoto University, Kyoto, Japan) per day post MI.^{21,22} In total, 68 wild-type (WT), 68 hSCF/tTA, and 24 ROSA^{mTmG};Wt1^{CreER} mice were used for *in vivo* experiments. Each EPDC culture was from 12 to 16 hearts of postnatal day 0 (P0) or embryonic day 13.5 (E13.5) mice.

Myocardial Infarction

MI was induced by occlusion of the left main coronary artery.^{20,22} Briefly, mice were anesthetized using a ketamine (20 mg/kg) and xylazine (12.5 mg/kg) cocktail intramuscularly, intubated, and artificially ventilated. The adequacy of anesthesia was monitored by absence of withdrawal reflex to tail pinch. Subsequently, a left intercostal thoracotomy was performed and the left coronary artery was surgically ligated. To achieve *in vivo* adenoviral infection, 10⁷ transducing units of adenoviral vector-expressing recombinant hSCF (Ad-hSCF) or LacZ (Ad-LacZ) was injected directly into the peri-infarct myocardium immediately after coronary artery ligation. The infection efficiency was confirmed by Western blot analysis.

Epicardium-Derived Cell Culture

EPDCs were cultured as previously described.²³ Hearts were removed from P0 or E13.5 mice, cut into pieces, and plated onto 1% gelatin-coated culture dish (epicardial side facing down) in Dulbecco's modified eagle medium containing 15% fetal calf serum for 6 to 9 days. EPDCs migrated from the heart explants were used for further experiments. Passage 1 EPDCs were used to assess cell proliferation. Each well of a 24-well plate was seeded with 10⁴ EPDCs. Ad-hSCF or Ad-green fluorescent protein (Ad-GFP) was added at a concentration of 10 multiplicity of infection. After 24 hours, cells were trypsinized and counted by NucleoCounter (New Brunswick Scientific, Enfield, CT).

Neonatal Cardiomyocyte Culture

P0 mouse hearts were isolated and digested using liberase (Roche, Canada). Cardiomyocytes were obtained and cultured in 24-well plates according to the methods we described previously.^{24,25} To isolate *c-kit* cardiomyocytes, *c-kit*⁺ cells were eliminated by *c-kit* antibody (Santa Cruz, CA)-conjugated magnetic beads (Invitrogen, CA). Overexpression of hSCF in WT neonatal cardiomyocytes was accomplished through the adenoviral infection of Ad-hSCF. Viral vectors containing LacZ served as the controls. Cells were infected with adenoviruses at 10 multiplicity of infection for 4 hours and incubated for an additional 48 hours before further experiments.

Scratch Migration Assay

A scratch migration assay was performed using a modified protocol as previously described.²⁶ Briefly, enhanced green fluorescence protein positive (EGFP⁺) EPDCs were passed into the wells (10⁴ per well) containing cultured *c-kit* negative neonatal cardiomyocytes infected with Ad-hSCF or Ad-LacZ. After overnight seeding, a scratch was created with a p100 pipette tip. Cell debris was removed and culture medium was changed to serum-free Dulbecco's modified eagle medium. After 24 hours, fluorescent images were taken using a fluorescence microscope (Observer D1, Carl Zeiss, Germany), and percentage of scratch closure was quantified.

Transwell Migration Assay

A transwell system was used to investigate EPDC migration.²⁷ Neonatal cardiomyocytes infected with Ad-hSCF or Ad-LacZ were cultured in the lower compartment. EGFP⁺ EPDCs were isolated from EGFP transgenic mice (Stock No. 004353, Jackson Laboratory) at P0, and passage 1 cells (5 \times 10⁴) were subcultured into the transwell cell culture inserts (8- μ m diameter pores). After 24 hours of incubation in Dulbecco's modified eagle medium containing 1% fetal calf serum, cells on upper layer of the insert membrane were completely removed by a cotton swab. EGFP⁺ EPDCs migrated to the other side of membrane were imaged using a fluorescence microscope (Observer D1, Carl Zeiss, Germany) and quantified.

Real-Time Reverse Transcription-Polymerase Chain Reaction

Total mRNA was isolated with TRIzol reagent (Invitrogen, Grand Island, NY) as previously described.²⁰ cDNA was synthesized using Moloney murine leukemia virus reverse transcriptase and random primers. Real-time polymerase chain reaction was conducted using SYBR Green PCR Master Mix (Eurogentec, San Diego, CA). 28S rRNA was used as a loading control. The oligonucleotide primer sequences were as follows: transforming growth factor (TGF)- β 1, forward, CAC TGC TTC CCG AAT GTC TG, reverse, GCC CGA AGC GGA CTA CTA TG; soluble mouse SCF with exon 6, forward, GCT TTG CTT TTG GAG CCT TA, reverse, TGA AAT TCT CTC TCT TTC TGT T; vascular endothelial growth factor A (VEGF-A), forward, GAT TGA GAC CCT GGT GGA CAT C, reverse, TCT CCT ATG TGC TGG CTT TGG T; basic fibroblast growth factor, forward, CAA GGG AGT GTG TGC CAA CC, reverse, TGC CCA GTT CGT TTC AGT GC. Samples were amplified for 35 cycles using Eppendorf Mastercycler Real-Time PCR machine (Eppendorf, Hamburg, Germany). The mRNA levels in relation to 28S rRNA were determined using the comparative Ct method.^{20,25}

Immunohistochemistry

Paraffin sections of the heart were deparaffinized, hydrated, and rinsed in PBS. Antigen retrieval was achieved by microwaving the slides in 10 mmol/L sodium citrate buffer (pH 6.0) at 94°C for 12 minutes. After normal serum blocking, slides were incubated with primary antibodies followed by biotinylated secondary antibody. Color was developed using an ABC kit (Vector Laboratory, Burlingame, CA).²⁶ Nuclei were counterstained with hematoxylin. Quantification of epicardial Wt1⁺ cells was presented by epicardial Wt1⁺ cell number divided by epicardial length. The nuclear size of epicardial cell

was measured by the shortest distance of nuclei. Arteriole number per millimeter squared and length density (mm/mm³) in the entire peri-infarct area were evaluated.^{28,29} Wheat germ agglutinin conjugated with Texas red (10 μg/mL, 30 minutes room temperature; Sigma, St Louis, MO) was used to stain cell membrane and epicardial cell surface area was quantified.

Frozen tissue sections and cells cultured on cover glass were fixed in 4% paraformaldehyde. Endogenous fluorescence was bleached by incubation in 0.3% H₂O₂ at room temperature overnight in a UV box.¹² Primary antibodies were applied followed by fluorescent second antibodies. Nuclei were stained with Hoechst 33342. Images were taken using a fluorescence microscope (Observer D1, Carl Zeiss, Germany). Primary antibody used were Wt1 (1:300; Calbiochem, San Diego, CA); phosphorylated Smad2 (1:200; Cell Signaling Technology, Danvers, MA); smooth muscle actin (SMA, 1:1000; Sigma, St Louis, MO); GFP (1:2000) and hSCF (1:200) from Abcam, Cambridge, MA); epicardin (1:300), *c-kit* (1:300), and TGFβ receptor 2 (1:200) from Santa Cruz Biotechnology, Santa Cruz, CA.

Western Blot Analysis

Myocardial expression of hSCF in ROSA^{mTmG};Wt1^{CreER} mice after Ad-hSCF adenoviral infection was measured by Western blot analysis.³⁰

Briefly, 40 μg of protein was separated by 12% SDS-PAGE gel and transferred to nitrocellulose membranes, and the blots were probed with antibodies against hSCF (1:500; Abcam, Cambridge, MA), TGFβ1 (1:500; Cell Signaling, Danvers, MA), or α-actinin (1:2500; Sigma, St Louis, MO). Blots were then washed and probed with horseradish peroxidase-conjugated secondary antibodies (1:3000; Bio-Rad, Hercules, CA), and detected by using an enhance chemiluminescence detection method.

VEGF-A ELISA

VEGF-A protein expression in P0 EPDCs was determined by using VEGF-A ELISA kit (RAB0510, Sigma). Briefly, passage 1 EPDCs were infected with either Ad-hSCF or Ad-GFP for 48 hours. Cell lysate were harvested, and equal amount of proteins was loaded to an ELISA plate according to the manufacturer's instructions. Color was developed using 3,3',5,5'-tetra-methylbenzidine, and absorbance was measured at 450 nm.

Statistical Analysis

Data were expressed as mean±SEM and analyzed using GraphPad Prism (version 3.0, La Jolla, CA). For data with multiple groups,

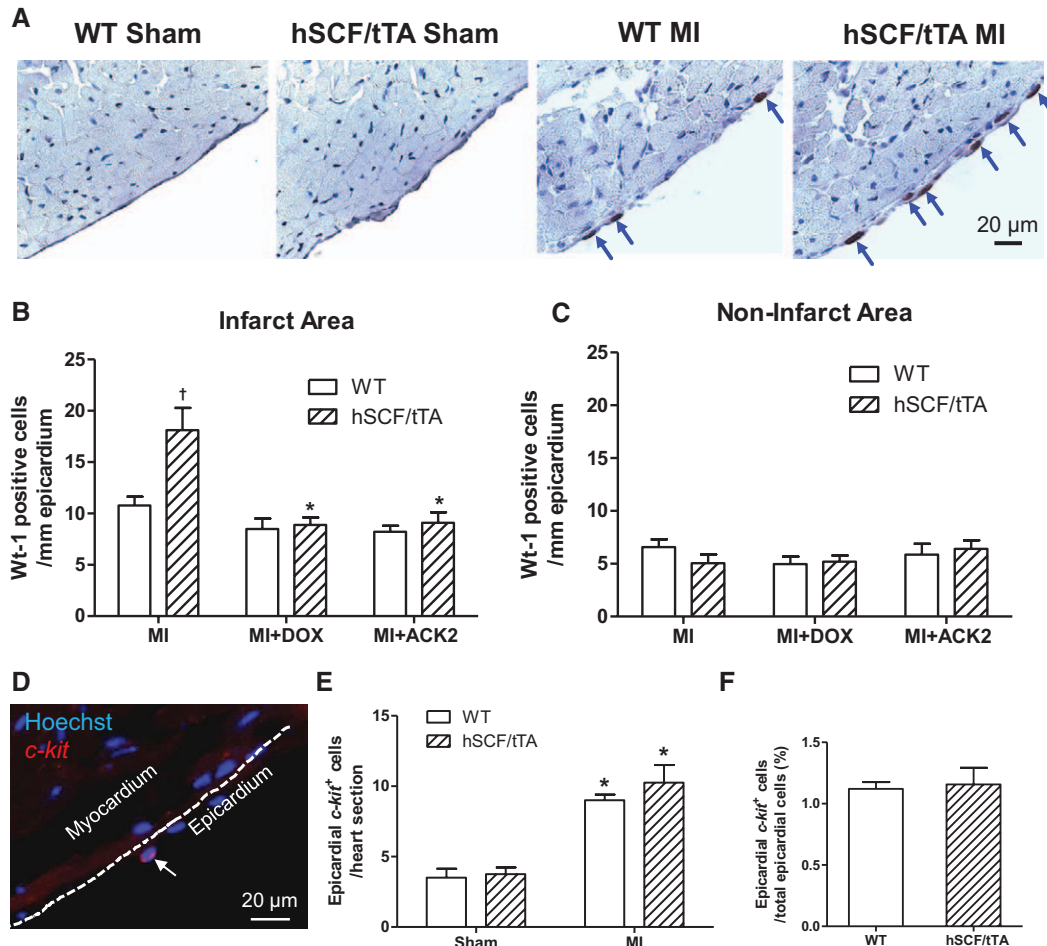


Figure 1. Epicardial Wilms tumor-1 (Wt1) expression 3 days post myocardial infarction (MI). **A**, Representative images of Wt1 staining. Wt1-positive cells have dark brown nuclear staining. Arrows point to Wt1-positive cells in the epicardium. **B** and **C**, Quantification of Wt1-positive cells in the epicardium. In the epicardium of infarct and peri-infarct area, significantly more epicardial Wt1⁺ cells were observed in human stem cell factor/tetracycline transactivator (hSCF/tTA) compared with wild-type (WT) mice 3 days post MI. This increase was abrogated by doxycycline (DOX) and ACK2 treatment. No significant changes were observed in the noninfarct area among all groups post MI (**C**). **D**, A representative image of *c-kit* staining in the epicardium. **E**, Quantification of epicardial *c-kit*⁺ cells. The population of *c-kit*⁺ epicardial cells significantly increased post MI in both WT and hSCF/tTA mice. **F**, The ratio of *c-kit*⁺ to total epicardial cells in WT and hSCF/tTA mice were similar, around 1.1%. **B** and **C**, n=6 to 7 per group. *P<0.05 vs hSCF/tTA MI, [†]P<0.05 vs WT MI. **E** and **F**, n=4 per group. *P<0.05 vs respective Sham (**E**); P=ns (**F**).

2-way ANOVA was performed followed by Bonferroni corrections, which were set for all possible pairwise comparisons. Wilcoxon rank-sum test was used to confirm findings from ANOVA. Results were not presented when they were agreeable with those from ANOVA. Unpaired Student *t* test was used for 2 group comparisons. A 2-tailed *P* value <0.05 was considered to be statistically significant.

Results

Epicardial Activation 3 Days Post MI

WT and hSCF/tTA mice were subjected to coronary artery ligation to induce MI. Three days after surgery, animals were euthanized and heart sections were immune-stained for Wt1, a specific marker for epicardial activation (Figure 1A). The number of Wt1⁺ cells in the epicardial layer was barely detectable in sham surgeries in WT and hSCF/tTA mice (0.36 ± 0.05 versus 0.33 ± 0.04 cells/mm; *n*=6 per group; *P*=ns). Three days post MI, the number of Wt1⁺ cells was increased to 5 to 10 cells/mm epicardium in WT mice (Figure 1A–1C). Furthermore, the population of Wt1⁺ cells in hSCF/tTA mice was almost doubled (18 cells/mm) in the epicardium of the infarct area (including the peri-infarct area) compared with WT (*P*<0.05; Figure 1B). Treatment with either doxycycline to turn off hSCF expression or ACK2 to block the SCF/*c-kit* signaling abrogated this response (*P*<0.05; Figure 1B). The number of Wt1⁺ cells was similar in the noninfarct area between hSCF/tTA and WT mice (Figure 1C). Also, few Wt1⁺ cells were observed in the myocardium post MI (Figure 1A)

as Wt1 expression is turned off after EMT.^{13–15,31} Notably, the nuclear size of epicardial cells was significantly increased in the infarct area post MI compared with sham groups in both WT and hSCF/tTA mice (*P*<0.05; Figure II in the Data Supplement); however, no significant difference was found in their nuclear or cell size between WT and hSCF/tTA MI mice (Figure II in the Data Supplement). *C-kit*⁺ epicardial cells have been shown to have stem cell potential.¹⁶ Thus, we performed *c-kit* staining to investigate the *c-kit*⁺ epicardial cell population. Expression of SCF receptor *c-kit* was found in epicardial cells (Figure 1D). Overlapping signals between *c-kit* and a membrane marker wheat germ agglutinin suggest that *c-kit* receptors are expressed on the epicardial cell membrane (Figure III in the Data Supplement). The total number of epicardial *c-kit*⁺ cells per heart section was significantly increased post MI (*P*<0.05; Figure 1E) and was equal to $\approx 1\%$ of epicardial cells (Figure 1F), which is consistent with previous studies.¹⁶ However, there was no significant difference between WT and hSCF/tTA mice (Figure 1E and 1F).

TGFβ1 is a key regulator of the EMT process. To assess its expression, TGFβ1 mRNA and protein levels in the epicardium and subepicardium of the peri-infarcted area were determined. Consistent with previous studies,^{32,33} we found that expression of TGFβ1 mRNA and protein were significantly higher post MI compared with sham groups (*P*<0.05; Figure 2A and 2B). Our data further showed that TGFβ1 expression in the epicardial and subepicardial tissues was

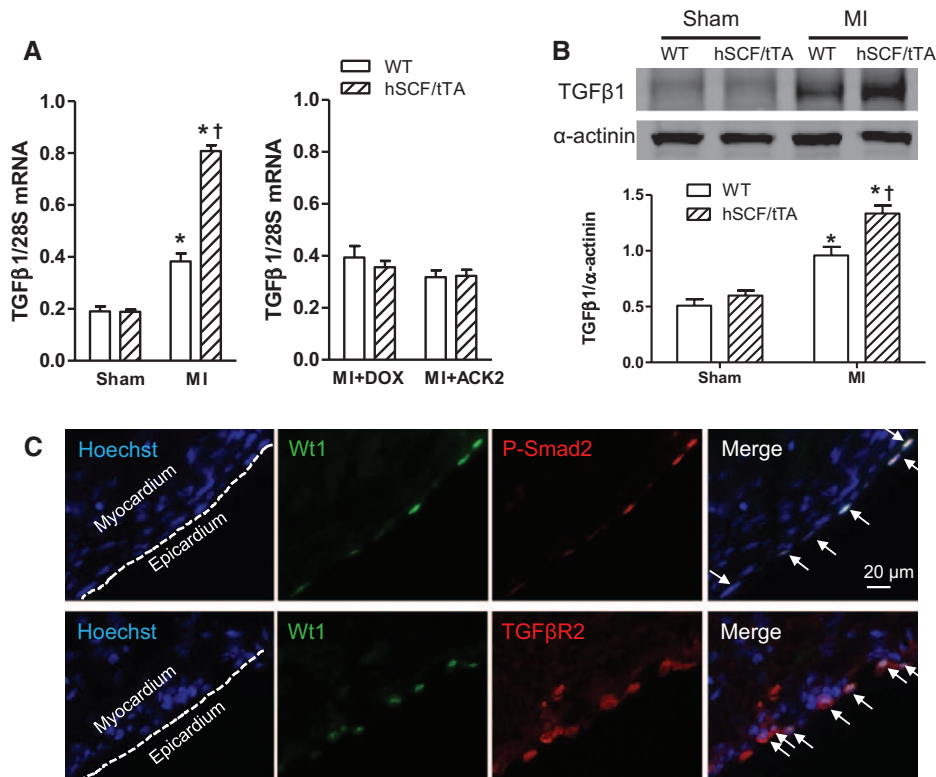


Figure 2. Myocardial transforming growth factor (TGF)-β expression and signaling in the epicardium 3 days post myocardial infarction (MI). **A**, There was significantly higher TGFβ mRNA expression in human stem cell factor/tetracycline transactivator (hSCF/tTA) mice compared with wild-type (WT) post MI. This difference was abrogated by doxycycline (DOX) and ACK2 treatment. **B**, There was also significantly higher TGFβ protein expression in hSCF/tTA mice compared with WT post MI. **C**, Representative images of Wilms tumor-1 (Wt1)/phosphor-Smad2 (P-Smad2) and Wt1/TGFβR2 staining in the epicardium 3 days post MI. P-Smad2 and TGFβR2 expression was observed in all epicardial Wt1⁺ cells. *n*=4 to 6 per group. **P*<0.05 vs respective Sham, †*P*<0.05 vs WT MI.

significantly higher in the peri-infarct area of hSCF/tTA compared with WT mice ($P<0.05$; Figure 2A and 2B), and the response was abolished by either doxycycline or ACK2 treatment ($P<0.05$; Figure 2A). As expected, Wt1⁺ epicardial cells were also positive for TGF β receptor 2 (TGF β R2) and nuclear phosphor-Smad2 3 days post MI (Figure 2C), indicating activation of TGF β 1 signaling.

Arteriole Density in Peri-Infarct Area 5 Days Post MI

EPDCs are essential for coronary artery formation during embryonic development.^{23,31} To investigate the effects of enhanced epicardial activation on arteriogenesis post MI, SMA staining was used to stain smooth muscle cells, and the number of arterioles (size between 15 and 150 μ m) was quantified in the whole peri-infarct area. Length density of arterioles was also calculated to evaluate the arteriolar bed independent of vessel orientations.^{28,29} Representative photomicrographs of SMA staining are presented in Figure 3A. Each arrow is pointing to an arteriole. Arteriole density was similar 5 days after sham surgery between WT and hSCF/tTA mice (Figure 3B). However, 5 days post MI, arteriole number and length density in the peri-infarct area were significantly higher in hSCF/tTA compared with WT mice ($P<0.05$; Figure 3B and 3C). Furthermore, the response was abrogated by doxycycline or ACK2 treatment ($P<0.05$; Figure 3B), suggesting SCF/*c-kit* signaling promotes myocardial arteriogenesis post MI.

Outgrowth of Cultured EPDCs

EPDCs can outgrow from P0 heart explants culture and form a monolayer of cobblestone-shaped cells (Figure IVA in the Data Supplement). The purity of EPDCs was confirmed by immunostaining of epicardin and Wt1, which are EPDC-specific markers (Figure IVB in the Data Supplement). Moreover, $\approx 3\%$ to 5% of the EPDCs were also positive for *c-kit* (Figure IVB in the Data Supplement). To study the effects of SCF on outgrowth of EPDCs, heart tissue sections from P0 WT mice were cultured and randomly divided into 2 treatment groups: control or recombinant mouse SCF (100 ng/mL). Six days after culturing, outgrowth of EPDCs from the heart tissue was observed (Figure 4A). Treatment with recombinant mouse SCF resulted in a significant higher EPDC outgrowth compared with controls ($P<0.05$; Figure 4B).

Proliferation and Proangiogenic Growth Factor Expression of Cultured EPDCs

Cultured EPDCs isolated from P0 hearts of WT mice were treated with Ad-hSCF or Ad-GFP. The expression of hSCF protein after Ad-hSCF infection was confirmed by Western blot analysis (data not shown). After 24 hours of treatment, EPDC cell numbers were significantly increased in the Ad-hSCF group compared with Ad-GFP control group ($P<0.05$; Figure 4C). Treatment with ACK2 (10 μ g/mL) significantly decreased EPDC cell numbers in both Ad-hSCF and Ad-GFP groups ($P<0.05$; Figure 4C). To investigate proangiogenic growth factor expression, cultured EPDCs from P0 hearts

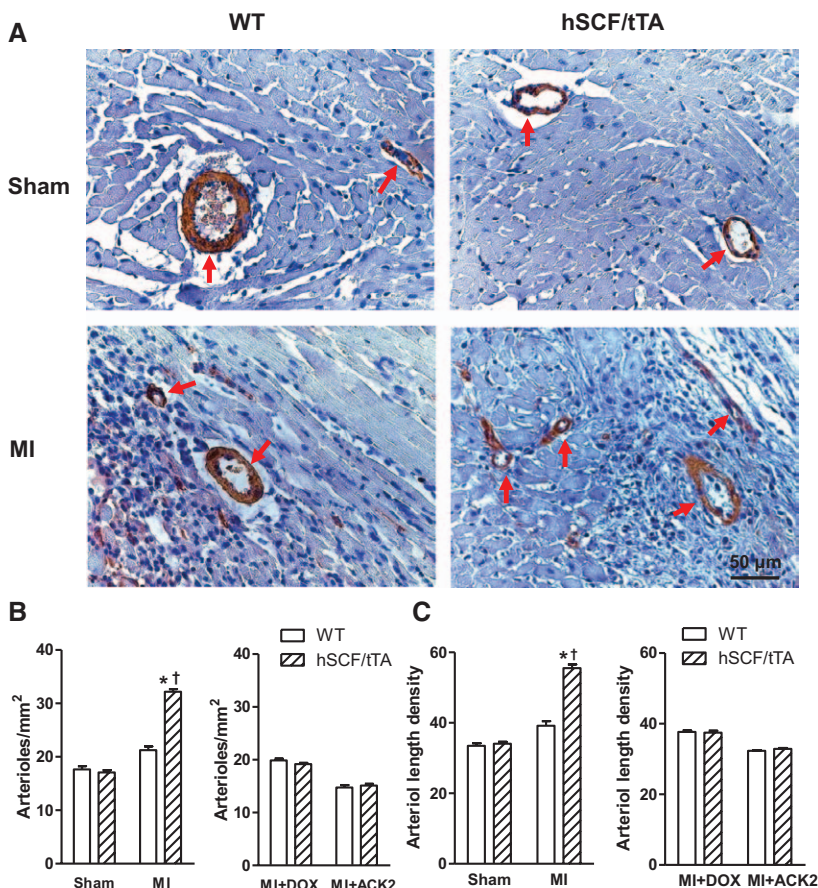


Figure 3. Arteriole density in the peri-infarct area post myocardial infarction (MI). **A**, Representative images of α -smooth muscle actin staining. Arterioles were identified as small vessels surrounded by smooth muscle actin positive cells. Arrows point to an arteriole. **B**, Quantification of arteriole density. Number of arterioles was significantly higher in the peri-infarct area of human stem cell factor/tetracycline transactivator (hSCF/tTA) compared with wild-type (WT) mice 5 days post MI, which was abrogated by doxycycline (DOX) and ACK2 treatment. **C**, Quantification of arteriole length density (mm/mm^3). Arteriole length density was significantly higher in the peri-infarct area of hSCF/tTA compared with WT mice 5 days post MI. $n=5$ per group. * $P<0.05$ vs respective Sham, † $P<0.05$ vs WT MI.

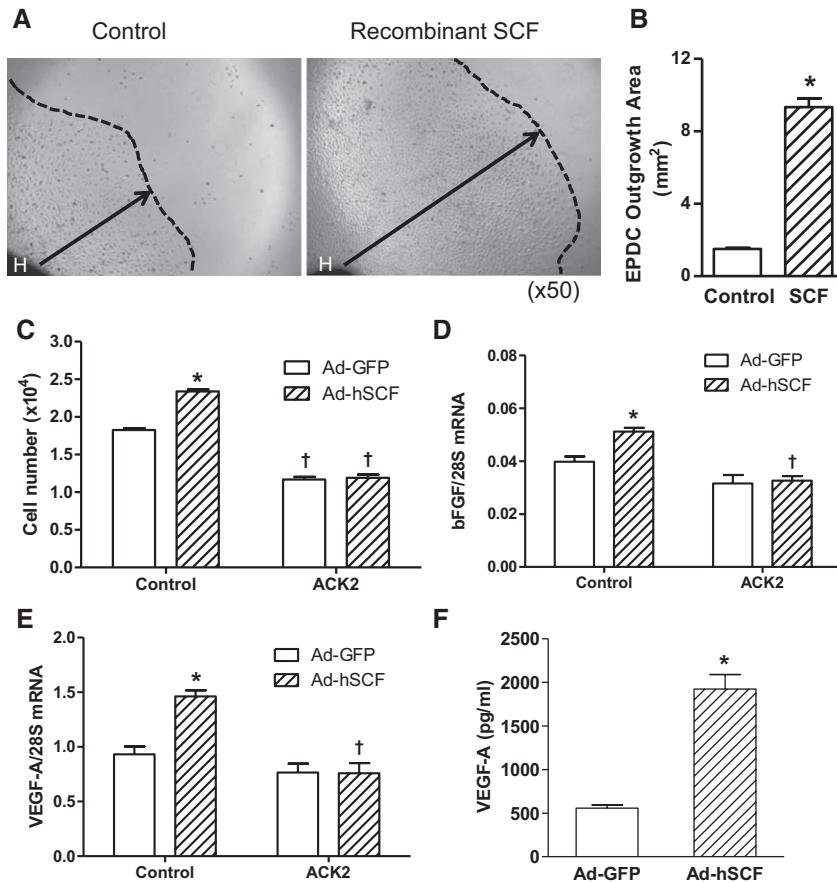


Figure 4. Outgrowth, proliferation, and growth factors expression in cultured epicardium-derived cells (EPDCs). **A**, Representative images showing EPDC outgrowth from the postnatal day 0 (P0) heart explants (H). Arrows indicate the EPDC migration distance from the heart explants. **B**, Recombinant mouse stem cell factor (SCF) treatment (100 ng/mL) significantly increased the EPDC outgrowth compared with control group. **C**, Overexpression of human SCF (hSCF) by adenoviral (Ad)-hSCF infection significantly increased proliferation of P0 EPDCs compared with Ad-green fluorescent protein (GFP) group. ACK2 treatment (10 μ g/mL) inhibited EPDC proliferation in both groups. **D** and **E**, Basic fibroblast growth factor (bFGF) and vascular endothelial growth factor (VEGF)-A mRNA levels in EPDCs were significantly increased by Ad-hSCF treatment compared with Ad-GFP. This effect was abolished by ACK2. **F**, VEGF-A protein expression in EPDCs was measured by ELISA. Overexpression of hSCF induced significantly higher VEGF-A protein expression compared with Ad-GFP control. $n=4$ to 7 per group, * $P<0.05$ vs control or Ad-GFP control, † $P<0.05$ vs respective control.

of WT mice were treated with Ad-GFP or Ad-hSCF for 24 hours. VEGF-A and basic fibroblast growth factor mRNA levels were significantly increased in the Ad-hSCF group compared with Ad-GFP control group ($P<0.05$; Figure 4D and 4E). Treatment with ACK2 (10 μ g/mL) abrogated this effect (Figure 4D and 4E). Furthermore, overexpression of hSCF significantly increased VEGF-A protein expression in EPDCs as determined by ELISA ($P<0.05$; Figure 4F). Interestingly, significantly more *c-kit*⁺ EPDCs were observed after the overexpression of hSCF, which may contribute to the enhanced EPDC proliferation and proangiogenic growth factor expression ($P<0.05$; Figure V in the Data Supplement).

Migration of Cultured EPDCs

To study the direct effect of hSCF overexpression in cardiomyocytes on EPDC migration, a scratch migration assay was performed in cardiomyocyte and EPDC cocultures. EGFP⁺ EPDCs were cocultured overnight with *c-kit*⁺ neonatal cardiomyocytes infected with Ad-LacZ or Ad-hSCF. A scratch was then induced (Figure 5A). Twenty-four hours later, a significantly higher scratch closure ratio by EGFP⁺ EPDCs was found in Ad-hSCF-treated cardiomyocytes compared with Ad-LacZ-treated controls ($P<0.05$; Figure 5B), suggesting overexpression of hSCF in cardiomyocytes directly promotes EPDC migration in the coculture.

A transwell assay was also used to study the effect of hSCF overexpression on EPDC migration.²⁷ EGFP⁺ EPDCs were seeded on the upper inserts with 8- μ m pores. Neonatal

cardiomyocytes infected with either Ad-LacZ or Ad-hSCF were seeded on the lower chamber. Cells were allowed to migrate for 24 hours, and the number of EGFP⁺ EPDCs, which had migrated through the insert membrane, was detected under fluorescent microscopy. As shown in Figure VI in the Data Supplement, the green cells are EGFP⁺ EPDCs, which had migrated through the membrane. Quantitative analysis showed that Ad-hSCF significantly increased EPDC migration compared with Ad-LacZ ($P<0.05$; Figure 5C). Furthermore, inhibition of *c-kit* signaling by ACK2 (10 μ g/mL) significantly attenuated EPDC migration in both Ad-LacZ and Ad-hSCF treatment groups ($P<0.05$; Figure 5C). The data indicate that EPDC migration is enhanced by chemokine release from the Ad-hSCF-treated neonatal cardiomyocytes in the lower chamber.

The *c-kit*⁺ progenitors exist in the neonatal heart.^{34,35} Activation of progenitor cells leads to release of multiple cytokines, growth factors, and chemokines, including soluble SCF.³⁶ Thus, we measured soluble mouse SCF in neonatal cardiomyocytes treated with Ad-hSCF or Ad-LacZ. As expected, soluble mouse SCF expression was significantly higher in hSCF overexpressing cardiomyocytes compared with Ad-LacZ group ($P<0.05$; Figure 5D), which was abrogated by ACK2 treatment ($P<0.05$; Figure 5D).

Lineage Tracing of Wt1⁺ EPDCs

EPDC activation and migration into the myocardium post MI was further investigated by lineage tracing of Wt1⁺ EPDCs.

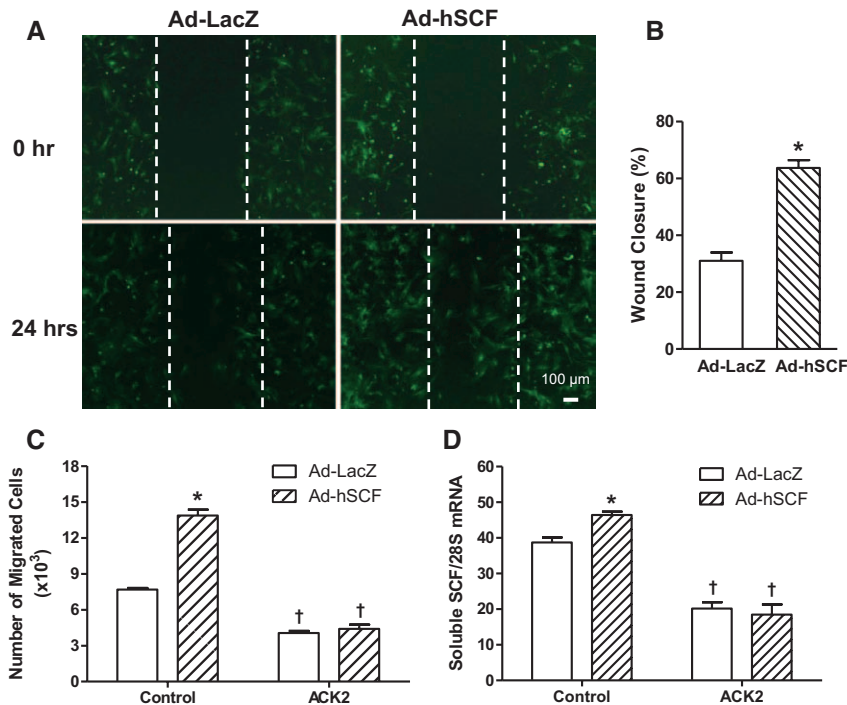


Figure 5. Epicardium-derived cell (EPDC) migration by scratch and transwell migration assays. **A**, Representative images of the scratch closure in cardiomyocyte-EGFP⁺ EPDC coculture. **B**, Quantification of scratch closure ratio at 24 hours, which was higher in the adenoviral human stem cell factor (Ad-hSCF) group (n=6 per group). * $P < 0.05$ vs Ad-LacZ. **C**, Quantification of EGFP⁺ EPDC migration through the transwell membrane, which was higher in the Ad-hSCF group and attenuated by ACK2. **D**, Expression of soluble mouse SCF mRNA in neonatal cardiomyocytes, which was higher in the Ad-hSCF group and attenuated by ACK2. n=3 per group for **C** and **D**. * $P < 0.05$ vs Ad-LacZ control, † $P < 0.05$ vs respective control.

Cre activation was induced by tamoxifen injection for 5 days before MI in ROSA^{mTmG};Wt1^{CreER} mice (Figure 6A). Five days post MI, 70% to 80% of the Wt1⁺ cells expressed EGFP, whereas all EGFP⁺ cells in the epicardium were Wt1⁺ (data not shown). Myocardial overexpression of hSCF in ROSA^{mTmG};Wt1^{CreER} mice was induced by intramyocardial injection of Ad-hSCF in the peri-infarct area immediately after coronary artery ligation. The expression of hSCF protein in the peri-infarct area 5 days post MI was detected by Western blot analysis (Figure VII in the Data Supplement). EGFP⁺ cells representing EPDCs derived from Wt1-expressing cells were found in the epicardium 5 days post MI (Figure 6B), which is consistent with our findings in Figure 1A and 1B. Importantly, EGFP⁺ cells were also observed in the infarcted myocardium (Figure 6C), providing direct evidence that Wt1⁺ EPDCs are activated and migrated into the infarct area. Furthermore, treatment with Ad-hSCF significantly increased the number of EGFP⁺ cells in the epicardium and infarcted myocardium compared with Ad-LacZ ($P < 0.05$; Figure 6D and 6E), which was abrogated by ACK2. Additionally, Ad-hSCF increased epicardial expression of TGF β , a key factor in promoting EMT, and the effect was also abrogated by ACK2 treatment (Figure 6F).

Wt1⁺ EPDC Differentiation

EPDCs contribute to coronary artery formation during embryonic heart development mainly by differentiating into vascular cells.³¹ To demonstrate the ability of EPDCs to differentiate, epicardial cells were cultured from hearts of ROSA^{mTmG};Wt1^{CreER} mice at P0. Treatment with tamoxifen (200 nmol/L) in the cultured ROSA^{mTmG};Wt1^{CreER} EPDCs showed 60% to 70% of Cre activation, resulting in EGFP expression in Wt1⁺ EPDCs (Figure VIIIA in the Data Supplement). The Wt1⁺ EPDCs were also differentiated into SMA⁺

cells (Figure VIIIB in the Data Supplement). So our next aim was to determine the lineage of Wt1-expressing cells in the infarct area post MI in ROSA^{mTmG};Wt1^{CreER} mice after tamoxifen treatment. As shown in Figure 7A, some of the EGFP⁺ cells in the infarct area were also positive for SMA, a marker for smooth muscle cells and myofibroblasts, indicating that Wt1⁺ EPDCs are able to differentiate into smooth muscle cells or myofibroblasts. Furthermore, treatment with Ad-hSCF significantly increased the total number of EGFP/SMA double-positive cells (Figure 7B) and total EGFP⁺ cells (Figure 7C). However, the percentage of EGFP⁺/SMA⁺ cells to total EGFP⁺ cells ($\approx 34\%$) in the infarcted myocardium was similar between Ad-LacZ- and Ad-hSCF-treated groups (Figure 7D), indicating Ad-hSCF treatment does not affect EPDC differentiation. Additionally, no SMA⁺ cells from the Wt1⁺ cell lineage were detected in any vessels in the peri-infarct area. Consistent with previous studies,³⁷ more than half of the EGFP⁺ cells in the infarct area were also positive for fibroblast marker FSP1 (Figure IX in the Data Supplement).

Discussion

The present study demonstrates for the first time that cardiomyocyte-specific expression of membrane-associated hSCF promotes epicardial activation post MI. The hSCF transgene expression increases epicardial Wt1⁺ EPDCs and arteriogenesis post MI. These effects are specific to membrane-associated hSCF because they are abrogated on treatment with doxycycline, which turns off hSCF expression on the membrane of cardiomyocytes. Moreover, through Wt1 lineage tracing, we showed that hSCF overexpression via adenoviral infection enhances EPDC activation and migration into the infarct area post MI through the *c-kit* signaling pathway. Furthermore, hSCF stimulates EPDCs to express VEGF and basic fibroblast

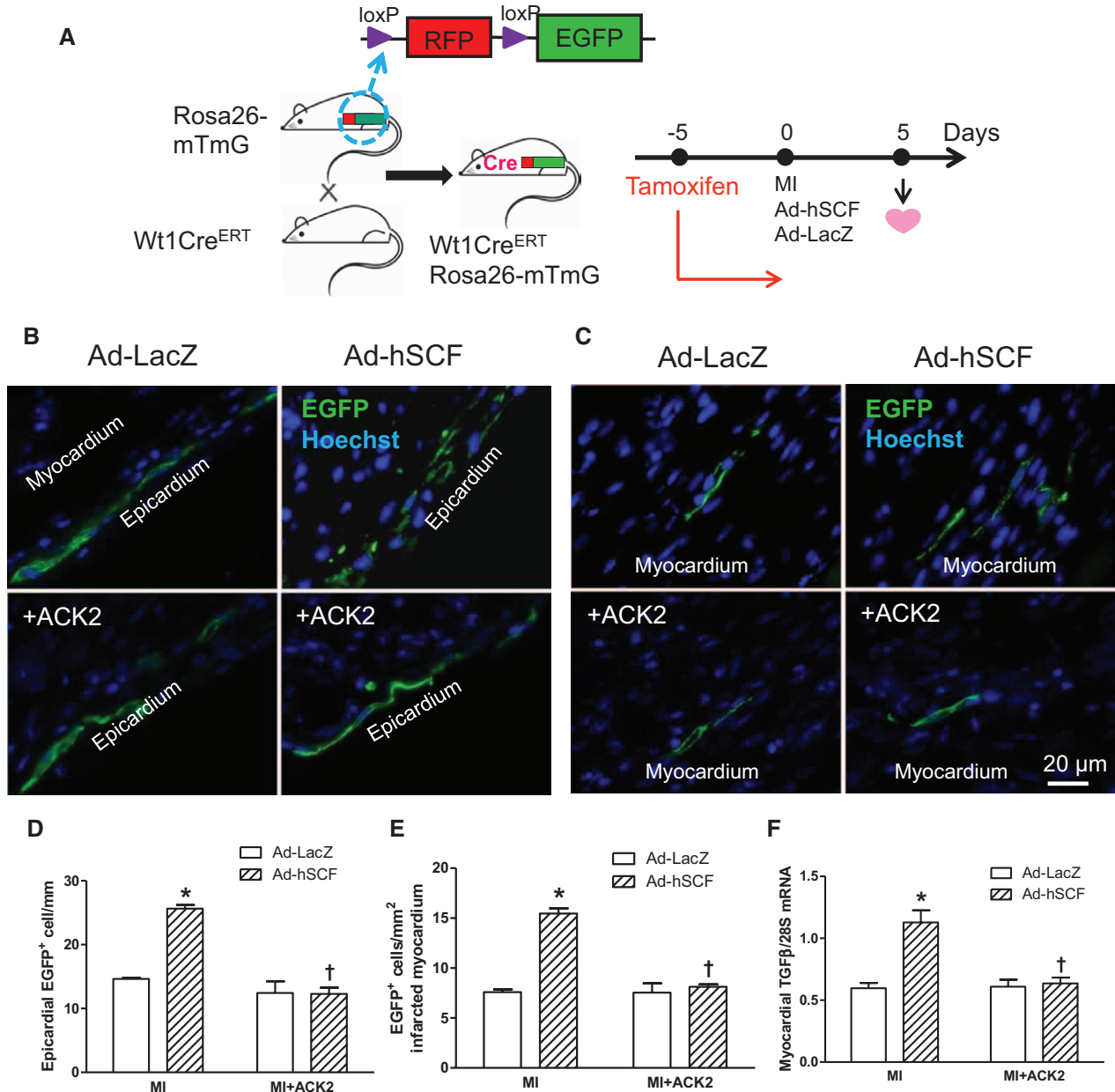


Figure 6. Lineage tracing of Wt1⁺ cell-derived epicardium-derived cells (EPDCs) 5 days post myocardial infarction (MI). **A**, Experimental outline for genetic fate mapping in the adult heart using ROSA^{mTmG};Wt1^{CreERT} mice. Representative images of EGFP staining in the epicardium (**B**) and infarcted myocardium (**C**) 5 days post MI. Quantification of EGFP⁺ cells in the epicardium (**D**) and infarcted myocardium (**E**). The number of Wt1⁺ cell-derived EPDCs was significantly higher in the epicardium and infarcted myocardium in the adenoviral human stem cell factor (Ad-hSCF)-treated group compared with Ad-LacZ 5 days post MI. ACK2 treatment abolished the difference in EGFP⁺ cells in the heart. **F**, Transforming growth factor (TGFβ) mRNA expression determined by real-time reverse transcription-polymerase chain reaction. In vivo Ad-hSCF treatment in the myocardium significantly increased TGFβ mRNA expression post MI. This increase was abrogated by ACK2. n=6 per group. *P<0.05 vs Ad-LacZ MI, †P<0.05 vs Ad-hSCF MI.

growth factor, which are important growth factors in arteriogenesis. These data show that hSCF overexpression enhances epicardial activation, EPDC production, and arteriogenesis post MI. We recently reported that cardiac-specific hSCF overexpression improves cardiac function and survival post MI.²⁰ The present study provides further insight into the cellular and molecular mechanisms of hSCF to improve cardiac repair post MI.

The adult epicardium can be reactivated and express Wt1 post MI.³⁷ In the present study, epicardial activation

as determined by Wt1 positivity was observed 3 days post MI, which is consistent with previous studies.^{37–39} Our novel finding is that overexpression of hSCF significantly enhanced the epicardial activation post MI, and the response was abrogated by inhibiting *c-kit* receptor function, suggesting an important role of SCF/*c-kit* signaling in epicardial activation. TGFβ1, one of the paracrine factors produced by stem/progenitor cells, has been shown to promote EMT in both embryonic and adult EPDCs.⁴⁰ A significant increase of TGFβ expression was found in the epicardium of hSCF

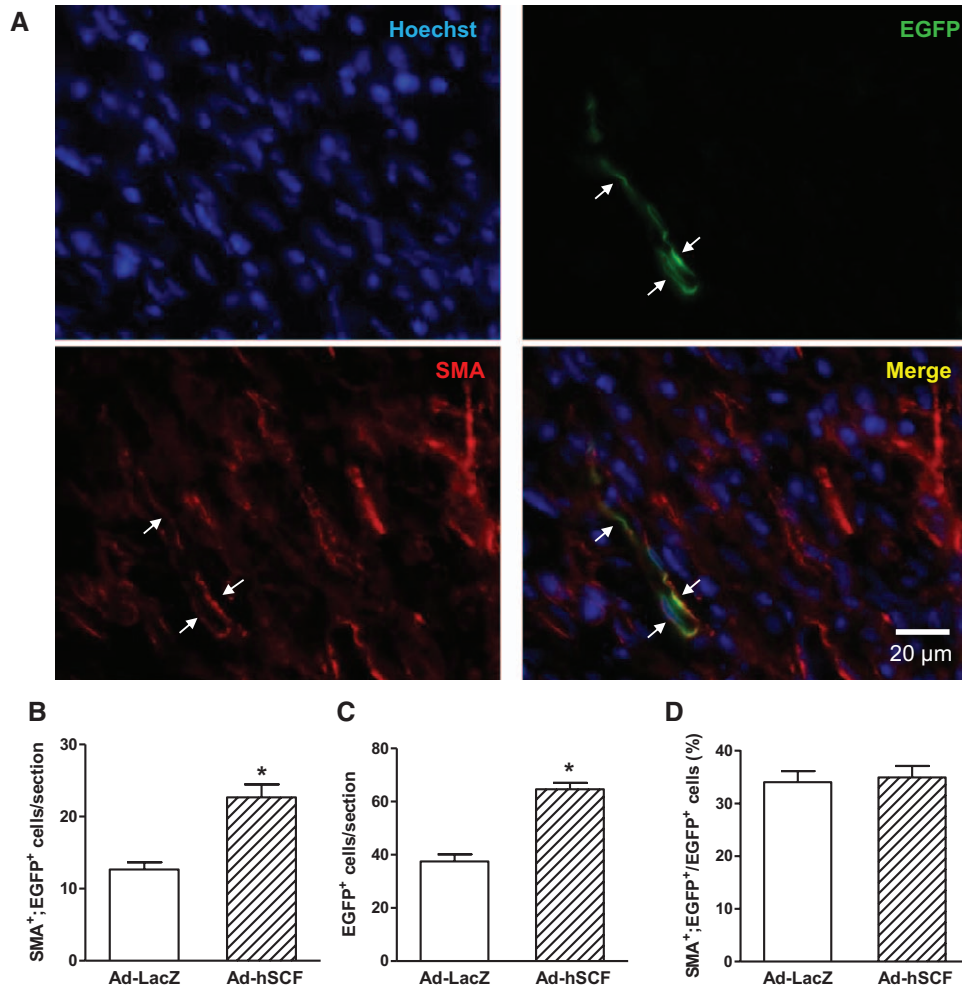


Figure 7. Fate mapping of Wt1⁺ cell-derived epicardium-derived cells (EPDCs) post myocardial infarction (MI). **A**, Representative images of EGFP and smooth muscle actin (SMA) staining of Wilms tumor-1-derived EPDCs in the infarcted myocardium. The EGFP⁺ cells are also positive for SMA (arrows). **B**, Quantification of the SMA⁺/EGFP⁺ (double positive) cells in the infarcted myocardium. The number of SMA⁺/EGFP⁺ cells was higher in adenoviral human stem cell factor (Ad-hSCF)-treated myocardium compared with Ad-LacZ. **C**, Quantification of the EGFP⁺ cells in the infarcted myocardium. The number of EGFP⁺ cells was higher with Ad-hSCF-treatment compared with Ad-LacZ. **D**, Percent SMA⁺/EGFP⁺ to total EGFP⁺ cells were not significantly different between Ad-hSCF and Ad-LacZ treatment. n=6 per group. *P<0.05 vs Ad-LacZ.

overexpressing mice post MI, and the effect was attenuated by doxycycline treatment to turn off hSCF expression or ACK2 treatment to inhibit *c-kit* receptor function, which suggests that activation of SCF/*c-kit* signaling enhances TGF β expression. Furthermore, TGF β 2 expression and nuclear Smad2 phosphorylation was observed in epicardial Wt1⁺ cells, suggesting activation of TGF β signaling in Wt1⁺ epicardial cells post MI. Expression of TGF β 2 was not observed in *c-kit*⁺ epicardial cells through fluorescent double staining (Figure X in the Data Supplement), indicating that TGF β may not directly act on *c-kit*⁺ epicardial cells.

The embryonic epicardium contributes to coronary artery formation.^{4,41} To assess the effects of enhanced epicardial activation by cardiac-specific overexpression of hSCF on arteriogenesis post MI, myocardial arteriole density was determined. Our data showed that hSCF overexpression significantly increased arteriole density in the peri-infarct area, suggesting a potential contribution of epicardial activation to arteriogenesis post MI. To further investigate the

effect of SCF on EPDC activity, overexpression of hSCF was induced in cultured EPDCs. Our data showed that the ability of cultured EPDCs to proliferate and migrate was significantly enhanced by hSCF overexpression via *c-kit* signaling. Moreover, expression of VEGF-A and basic fibroblast growth factor, 2 well-known proangiogenic growth factors involved in arteriogenesis,^{42,43} was upregulated through the SCF/*c-kit* pathway, suggesting an enhanced paracrine effect of EPDCs. Although only 5% of cultured EPDCs and \approx 20 000 cells (or 0.65%) in the neonatal heart express *c-kit*,^{34,35} activation and expansion of those cells by hSCF may promote activation of many neighboring EPDCs by paracrine factors, which may further initiate signaling pathways to induce cell proliferation and migration. Additionally, the membrane-anchored hSCF on cardiomyocytes infected with Ad-hSCF also directly promotes EPDC migration as shown by a scratch migration assay.

To trace cell fate of the activated epicardium in vivo, a ROSA^{mTmG};Wt1^{CreER} mouse was generated, in which Cre

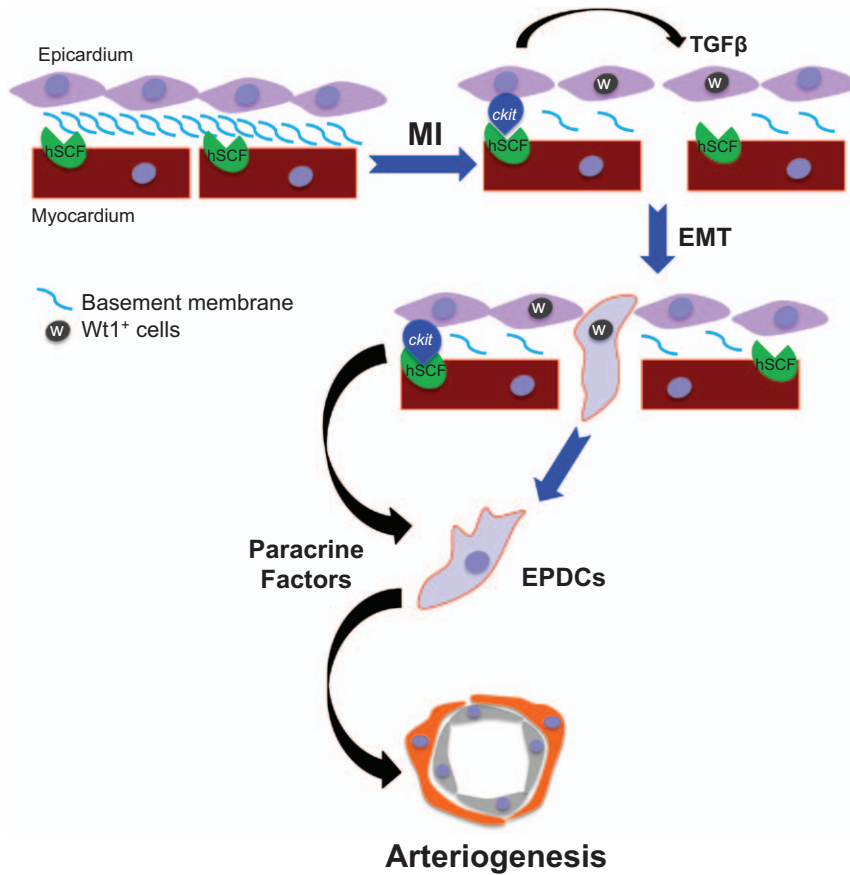


Figure 8. Schematic signaling pathways underlying epicardial activation and arteriogenesis in human stem cell factor/tetracycline transactivator (hSCF/tTA) mice post myocardial infarction (MI). Under basal conditions, the epicardium is not activated and hSCF expressed on the myocyte membrane does not have access to its receptor *c-kit*. After MI, however, the epicardium becomes activated by factors, such as transforming growth factor- β (TGF β). The *c-kit*⁺ epicardial cells are able to interact with hSCF on the myocyte membrane because of breakdown of epicardial basement membrane post MI,⁴⁵ leading to enhanced epicardial activation, epithelial–mesenchymal transition (EMT), and production of epicardial-derived cells (EPDC). EPDCs and other *c-kit*⁺ cells in response to hSCF stimulation release paracrine factors, including vascular endothelial growth factor, basic fibroblast growth factor, and possibly soluble SCF, and enhance arteriogenesis in the infarcted myocardium. Black arrows indicate paracrine effects.

recombinase expression is inducible by tamoxifen treatment and *Wt1* expression cells and their progeny will be EGFP⁺. Myocardial hSCF overexpression was achieved by intramyocardial injection of adenoviral hSCF constructs. Consistent with what we found in the hSCF/tTA mice, overexpression of hSCF by adenoviral infection enhanced epicardial activation post MI in ROSA^{mTmG}; *Wt1*^{CreER} mice as shown by a significantly higher number of EGFP⁺ epicardial cells. A hallmark of activated EPDCs is their ability to undergo EMT and migrate into the myocardium.¹⁷ Zhou et al³⁷ also investigated the migration of EPDCs using the same lineage tracing system. However, the EGFP⁺ EPDCs remained in the epicardial region and did not migrate into the myocardium. This is not surprising as their study was specifically designed to trace *Wt1*⁺ epicardial cells before the onset of MI. In the present study, we used a tamoxifen treatment protocol to turn on Cre recombinase activity at the peak of epicardial *Wt1* expression and were able to see EGFP⁺ cells in the infarcted myocardium 5 days post MI. More importantly, hSCF overexpression significantly increased the number of EGFP⁺ cells, which had migrated into the myocardium. A significant increase of TGF β mRNA expression was also observed post MI in the epicardium of Ad-hSCF–treated ROSA^{mTmG}; *Wt1*^{CreER} mice. Furthermore, increases in EPDC migration and TGF β expression were abrogated by the inhibition of *c-kit* signaling. Together, these data show that activation of SCF/*c-kit* signaling promotes EMT of *Wt1*⁺ EPDCs and their migration into the infarcted myocardium via upregulation of TGF β .

After EMT and migration into the myocardium during embryonic heart development, EPDCs differentiate into several cellular lineages, including cardiomyocytes, endothelial cells, smooth muscle cells, and interstitial fibroblasts.^{3,4,31} Although the adult epicardium can be reactivated post MI, cell fate of EPDCs remains to be determined. Through lineage tracing of *Wt1*⁺ EPDCs, we showed that the total number of EPDCs and their SMA⁺ derivatives were significantly increased by hSCF overexpression. However, their commitment to smooth muscle and myofibroblast lineages 5 days post MI was not altered by hSCF overexpression (Figure 7D). The SMA⁺ cell lineage was mainly found in the infarct area, whereas arteriogenesis was predominantly in the peri-infarct area. The fact that not a single artery is derived from the EPDC lineage suggests that the increased arteriogenesis by hSCF overexpression is mainly caused by paracrine effects. Of interest, lineage commitment of EPDCs post MI may be partially modified. To this end, Smart et al³⁸ successfully induced 0.6% of *Wt1*⁺ EPDCs differentiation into structurally coupled cardiomyocytes using thymosin β 4. However, this observation was not reproduced by Zhou et al.⁴⁴ In the present study, we did not observe any effects of hSCF overexpression on cardiomyocyte generation from the EPDCs. Most of the activated EPDCs differentiate into fibroblasts in the infarcted myocardium.

In summary, the present study shows that cardiac-specific hSCF overexpression enhances epicardial activation, EPDC production, growth factor expression, and arteriogenesis post MI (see Figure 8 for the proposed mechanism). These effects may contribute to a significant improvement in cardiac

function and survival in hSCF/tTA mice post MI.²⁰ Our study provides novel insight in EPDC activation post MI and suggests that cardiac-specific hSCF overexpression may have therapeutic potential in promoting cardiac repair post MI. Further translational studies are required to investigate the effects of hSCF by cardiac-specific gene therapy in large animal models of MI and in patients after acute MI.

Sources of Funding

This study was supported by an operating grant from the Canadian Institutes of Health Research (CIHR, MOP-64395 to Dr Feng). Dr Xiang was supported by a Doctoral Research Award from the Heart and Stroke Foundation of Canada (HSFC). Dr Feng is an HSFC Career Investigator.

Disclosures

None.

References

- Mensah GA, Brown DW. An overview of cardiovascular disease burden in the United States. *Health Affairs*. 2007;26:38–48.
- Ptaszek LM, Mansour M, Ruskin JN, Chien KR. Towards regenerative therapy for cardiac disease. *Lancet*. 2012;379:933–942.
- Cai CL, Martin JC, Sun Y, Cui L, Wang L, Ouyang K, Yang L, Bu L, Liang X, Zhang X, Stallcup WB, Denton CP, McCulloch A, Chen J, Evans SM. A myocardial lineage derives from Tbx18 epicardial cells. *Nature*. 2008;454:104–108.
- Zhou B, Ma Q, Rajagopal S, Wu SM, Domian I, Rivera-Feliciano J, Jiang D, von Gise A, Ikeda S, Chien KR, Pu WT. Epicardial progenitors contribute to the cardiomyocyte lineage in the developing heart. *Nature*. 2008;454:109–113.
- Smart N, Dubé KN, Riley PR. Coronary vessel development and insight towards neovascular therapy. *Int J Exp Pathol*. 2009;90:262–283.
- Winter EM, Grauss RW, Hogers B, van Tuyn J, van der Geest R, Lie-Venema H, Steijn RV, Maas S, DeRuiter MC, deVries AA, Steendijk P, Doevendans PA, van der Laarse A, Poelmann RE, Schalij MJ, Atsma DE, Gittenberger-de Groot AC. Preservation of left ventricular function and attenuation of remodeling after transplantation of human epicardium-derived cells into the infarcted mouse heart. *Circulation*. 2007;116:917–927.
- Männer J, Pérez-Pomares JM, Macías D, Muñoz-Chápuli R. The origin, formation and developmental significance of the epicardium: a review. *Cells Tissues Organs*. 2001;169:89–103.
- del Monte G, Casanova JC, Guadix JA, MacGrogan D, Burch JB, Pérez-Pomares JM, de la Pompa JL. Differential Notch signaling in the epicardium is required for cardiac inflow development and coronary vessel morphogenesis. *Circ Res*. 2011;108:824–836.
- Gittenberger-de Groot AC, Winter EM, Bartelings MM, Goumans MJ, DeRuiter MC, Poelmann RE. The arterial and cardiac epicardium in development, disease and repair. *Differentiation*. 2012;84:41–53.
- Wu B, Zhang Z, Lui W, Chen X, Wang Y, Chamberlain AA, Moreno-Rodriguez RA, Markwald RR, O'Rourke BP, Sharp DJ, Zheng D, Lenz J, Baldwin HS, Chang CP, Zhou B. Endocardial cells form the coronary arteries by angiogenesis through myocardial-endocardial VEGF signaling. *Cell*. 2012;151:1083–1096.
- Red-Horse K, Ueno H, Weissman IL, Krasnow MA. Coronary arteries form by developmental reprogramming of venous cells. *Nature*. 2010;464:549–553.
- von Gise A, Zhou B, Honor LB, Ma Q, Petryk A, Pu WT. WT1 regulates epicardial epithelial to mesenchymal transition through β -catenin and retinoic acid signaling pathways. *Dev Biol*. 2011;356:421–431.
- Pérez-Pomares JM, Phelps A, Sedmerova M, Carmona R, González-Iriarte M, Muñoz-Chápuli R, Wessels A. Experimental studies on the spatiotemporal expression of WT1 and RALDH2 in the embryonic avian heart: a model for the regulation of myocardial and valvuloseptal development by epicardially derived cells (EPDCs). *Dev Biol*. 2002;247:307–326.
- Moore AW, McInnes L, Kreidberg J, Hastie ND, Schedl A. YAC complementation shows a requirement for Wt1 in the development of epicardium, adrenal gland and throughout nephrogenesis. *Development*. 1999;126:1845–1857.
- Carmona R, González-Iriarte M, Pérez-Pomares JM, Muñoz-Chápuli R. Localization of the Wilm's tumour protein WT1 in avian embryos. *Cell Tissue Res*. 2001;303:173–186.
- Limana F, Zacheo A, Mocini D, Mangoni A, Borsellino G, Diamantini A, De Mori R, Battistini L, Vigna E, Santini M, Loiaconi V, Pompilio G, Germani A, Capogrossi MC. Identification of myocardial and vascular precursor cells in human and mouse epicardium. *Circ Res*. 2007;101:1255–1265.
- Limana F, Capogrossi MC, Germani A. The epicardium in cardiac repair: from the stem cell view. *Pharmacol Ther*. 2011;129:82–96.
- Smith MA, Court EL, Smith JG. Stem cell factor: laboratory and clinical aspects. *Blood Rev*. 2001;15:191–197.
- Friel J, Heberlein C, Itoh K, Ostertag W. Role of the stem cell factor (SCF) receptor and the alternative forms of its ligand (SCF) in the induction of long-term growth by stroma cells. *Leukemia*. 1997;11(suppl 3):493–495.
- Xiang FL, Lu X, Hammoud L, Zhu P, Chidiac P, Robbins J, Feng Q. Cardiomyocyte-specific overexpression of human stem cell factor improves cardiac function and survival after myocardial infarction in mice. *Circulation*. 2009;120:1065–1074.
- Nishikawa S, Kusakabe M, Yoshinaga K, Ogawa M, Hayashi S, Kunisada T, Era T, Sakakura T, Nishikawa S. In utero manipulation of coat color formation by a monoclonal anti-c-kit antibody: two distinct waves of c-kit-dependency during melanocyte development. *EMBO J*. 1991;10:2111–2118.
- Xiang FL, Lu X, Liu Y, Feng Q. Cardiomyocyte-specific overexpression of human stem cell factor protects against myocardial ischemia and reperfusion injury. *Int J Cardiol*. 2013;168:3486–3494.
- Liu Y, Lu X, Xiang FL, Poelmann RE, Gittenberger-de Groot AC, Robbins J, Feng Q. Nitric oxide synthase-3 deficiency results in hypoplastic coronary arteries and postnatal myocardial infarction. *Eur Heart J*. 2014;35:920–931.
- Zhang T, Lu X, Beier F, Feng Q. Rac1 activation induces tumor necrosis factor- α expression and cardiac dysfunction in endotoxemia. *J Cell Mol Med*. 2011;15:1109–1121.
- Zhang T, Lu X, Li J, Chidiac P, Sims SM, Feng Q. Inhibition of Na/K-ATPase promotes myocardial tumor necrosis factor- α protein expression and cardiac dysfunction via calcium/mTOR signaling in endotoxemia. *Basic Res Cardiol*. 2012;107:254.
- Moazzen H, Lu X, Ma NL, Velenosi TJ, Urquhart BL, Wisse LJ, Gittenberger-de Groot AC, Feng Q. N-Acetylcysteine prevents congenital heart defects induced by pregestational diabetes. *Cardiovasc Diabetol*. 2014;13:46.
- Li N, Lu X, Zhao X, Xiang FL, Xenocostas A, Karmazyn M, Feng Q. Endothelial nitric oxide synthase promotes bone marrow stromal cell migration to the ischemic myocardium via upregulation of stromal cell-derived factor-1 α . *Stem Cells*. 2009;27:961–970.
- Dedkov EI, Christensen LP, Weiss RM, Tomanek RJ. Reduction of heart rate by chronic β -adrenoceptor blockade promotes growth of arterioles and preserves coronary perfusion reserve in postinfarcted heart. *Am J Physiol Heart Circ Physiol*. 2005;288:H2684–H2693.
- Anversa P, Capasso JM. Loss of intermediate-sized coronary arteries and capillary proliferation after left ventricular failure in rats. *Am J Physiol*. 1991;260(5 pt 2):H1552–H1560.
- Zhang T, Lu X, Arnold P, Liu Y, Baliga R, Huang H, Bauer JA, Liu Y, Feng Q. Mitogen-activated protein kinase phosphatase-1 inhibits myocardial TNF- α expression and improves cardiac function during endotoxemia. *Cardiovasc Res*. 2012;93:471–479.
- Lie-Venema H, van den Akker NM, Bax NA, Winter EM, Maas S, Keekarainen T, Hoeben RC, deRuiter MC, Poelmann RE, Gittenberger-de Groot AC. Origin, fate, and function of epicardium-derived cells (EPDCs) in normal and abnormal cardiac development. *ScientificWorldJournal*. 2007;7:1777–1798.
- Deten A, Hölzl A, Leicht M, Barth W, Zimmer HG. Changes in extracellular matrix and in transforming growth factor β isoforms after coronary artery ligation in rats. *J Mol Cell Cardiol*. 2001;33:1191–1207.
- Wünsch M, Sharma HS, Markert T, Bernotat-Danielowski S, Schott RJ, Kremer P, Bleese N, Schaper W. In situ localization of transforming growth factor β 1 in porcine heart: enhanced expression after chronic coronary artery constriction. *J Mol Cell Cardiol*. 1991;23:1051–1062.
- Zaruba MM, Soonpaa M, Reuter S, Field LJ. Cardiomyogenic potential of C-kit(+)-expressing cells derived from neonatal and adult mouse hearts. *Circulation*. 2010;121:1992–2000.
- Tallini YN, Greene KS, Craven M, Speelman A, Breitbach M, Smith J, Fisher PJ, Steffey M, Hesse M, Doran RM, Woods A, Singh B, Yen

- A, Fleischmann BK, Kotlikoff MI. c-kit expression identifies cardiovascular precursors in the neonatal heart. *Proc Natl Acad Sci USA*. 2009;106:1808–1813.
36. Ratajczak MZ, Kucia M, Jadczyk T, Greco NJ, Wojakowski W, Tendera M, Ratajczak J. Pivotal role of paracrine effects in stem cell therapies in regenerative medicine: can we translate stem cell-secreted paracrine factors and microvesicles into better therapeutic strategies? *Leukemia*. 2012;26:1166–1173.
 37. Zhou B, Honor LB, He H, Ma Q, Oh JH, Butterfield C, Lin RZ, Melero-Martin JM, Dolmatova E, Duffy HS, Gise Av, Zhou P, Hu YW, Wang G, Zhang B, Wang L, Hall JL, Moses MA, McGowan FX, Pu WT. Adult mouse epicardium modulates myocardial injury by secreting paracrine factors. *J Clin Invest*. 2011;121:1894–1904.
 38. Smart N, Bollini S, Dubé KN, Vieira JM, Zhou B, Davidson S, Yellon D, Riegler J, Price AN, Lythgoe MF, Pu WT, Riley PR. De novo cardiomyocytes from within the activated adult heart after injury. *Nature*. 2011;474:640–644.
 39. Limana F, Bertolami C, Mangoni A, Di Carlo A, Avitabile D, Mocini D, Iannelli P, De Mori R, Marchetti C, Pozzoli O, Gentili C, Zacheo A, Germani A, Capogrossi MC. Myocardial infarction induces embryonic reprogramming of epicardial c-kit(+) cells: role of the pericardial fluid. *J Mol Cell Cardiol*. 2010;48:609–618.
 40. Bax NA, van Oorschot AA, Maas S, Braun J, van Tuyn J, de Vries AA, Groot AC, Goumans MJ. *In vitro* epithelial-to-mesenchymal transformation in human adult epicardial cells is regulated by TGF β -signaling and WT1. *Basic Res Cardiol*. 2011;106:829–847.
 41. Winter EM, Gittenberger-de Groot AC. Epicardium-derived cells in cardiogenesis and cardiac regeneration. *Cell Mol Life Sci*. 2007;64:692–703.
 42. Banai S, Jaklitsch MT, Shou M, Lazarous DF, Scheinowitz M, Biro S, Epstein SE, Unger EF. Angiogenic-induced enhancement of collateral blood flow to ischemic myocardium by vascular endothelial growth factor in dogs. *Circulation*. 1994;89:2183–2189.
 43. Lazarous DF, Scheinowitz M, Shou M, Hodge E, Rajanayagam S, Hunsberger S, Robison WG Jr, Stiber JA, Correa R, Epstein SE. Effects of chronic systemic administration of basic fibroblast growth factor on collateral development in the canine heart. *Circulation*. 1995;91:145–153.
 44. Zhou B, Honor LB, Ma Q, Oh JH, Lin RZ, Melero-Martin JM, von Gise A, Zhou P, Hu T, He L, Wu KH, Zhang H, Zhang Y, Pu WT. Thymosin beta 4 treatment after myocardial infarction does not reprogram epicardial cells into cardiomyocytes. *J Mol Cell Cardiol*. 2012;52:43–47.
 45. von Gise A, Pu WT. Endocardial and epicardial epithelial to mesenchymal transitions in heart development and disease. *Circ Res*. 2012;110:1628–1645.

CLINICAL PERSPECTIVE

Loss of myocardium and blood vessels after myocardial infarction (MI) results in scar formation and cardiac remodeling, leading to heart failure. Regeneration of the vascular system is critical to cardiac repair post MI. During embryonic heart development, epicardial-derived cells (EPDCs) contribute to coronary artery formation. In the adult heart, the epicardial cells can be reactivated post MI. However, the number of endogenously activated EPDCs is limited to efficiently repair the injured myocardium. We have previously shown that inducible cardiomyocyte-specific overexpression of membrane-associated human stem cell factor (hSCF) improves cardiac function post MI via myocardial angiogenesis. In the present study, we aim to investigate the effects of cardiomyocyte-specific overexpression of hSCF on EPDC activation and arteriogenesis after MI. We demonstrated that cardiomyocyte-specific hSCF overexpression increased EPDC activation and promoted myocardial arteriogenesis after MI. These beneficial effects are likely caused by enhanced activation, proliferation, and migration of EPDCs and release of paracrine factors by hSCF overexpression. This study highlights a therapeutic potential of hSCF in the treatment of MI and heart failure.

Cardiac-Specific Overexpression of Human Stem Cell Factor Promotes Epicardial Activation and Arteriogenesis after Myocardial Infarction

Fu-Li Xiang, Yin Liu, Xiangru Lu, Douglas L. Jones, Qingping Feng

Departments of Physiology and Pharmacology, and Medicine, Western University, Lawson Health Research Institute, London, Ontario, Canada.

Supplemental Figure Legends:

Suppl. Figure 1: Expression of hSCF protein in hSCF/tTA mice. **A.** hSCF staining showed the expression of hSCF was located on sarcolemma of cardiomyocytes in hSCF/tTA mice and was turned off by DOX treatment. A WT heart served as a negative control. **B.** In the serum of hSCF/tTA mice, S- hSCF was not detectable. Heart tissues from hSCF/tTA mice served as positive controls. MA-hSCF, membrane-associated hSCF; S-hSCF, soluble hSCF.

Suppl. Figure 2: Cell and nuclear size of epicardial cells. Three days after MI or sham surgery, nuclear size and cell surface area of epicardial cells was quantified. **A.** Significantly larger epicardial nuclei were observed in the MI compared to sham animals. No significant difference was found between WT and hSCF/tTA mice. Two-way ANOVA followed by Bonferroni corrections: $*P < 0.05$ vs respective sham. **B.** No significant difference of epicardial cell surface area was found between WT and hSCF/tTA mice. Unpaired Student *t*-test: $P = n.s.$ Data are mean \pm SEM, $n = 3-4$ per group.

Suppl. Figure 3: Identification of *c-kit* receptor on epicardial cell membrane. Representative images show that *c-kit* (green) receptors are located on the cell membrane (WGA, red) of *c-kit*⁺ epicardial cells.

Suppl. Figure 4: *In vitro* culture of EPDCs. **A.** 6 days after heart explants culture, cobblestone shaped cell monolayer was observed surrounding the heart explants. **B.** Cobblestone shaped cells outgrown from the heart explants were 100% positive for epicardin (nuclei: blue, epicardin: red) and Wt1 (nuclei: blue, Wt1: red). Some EPDCs were also positive for *c-kit* (nuclei: blue, *c-kit*: red).

Suppl. Figure 5: Overexpression of hSCF increases *c-kit*⁺ EPDCs *in vitro*. **A.** Representative images of cultured EPDCs 24 hours after Ad-hSCF or Ad-LacZ infection. *C-kit* was stained in green. **B.** Quantification of *c-kit*⁺ EPDC percentage. Overexpression of hSCF significantly increased the *c-kit*⁺ EPDC percentage *in vitro*. Data are mean \pm SEM, n=5 per group. Unpaired Student *t*-test: **P*<0.05 vs Ad-LacZ.

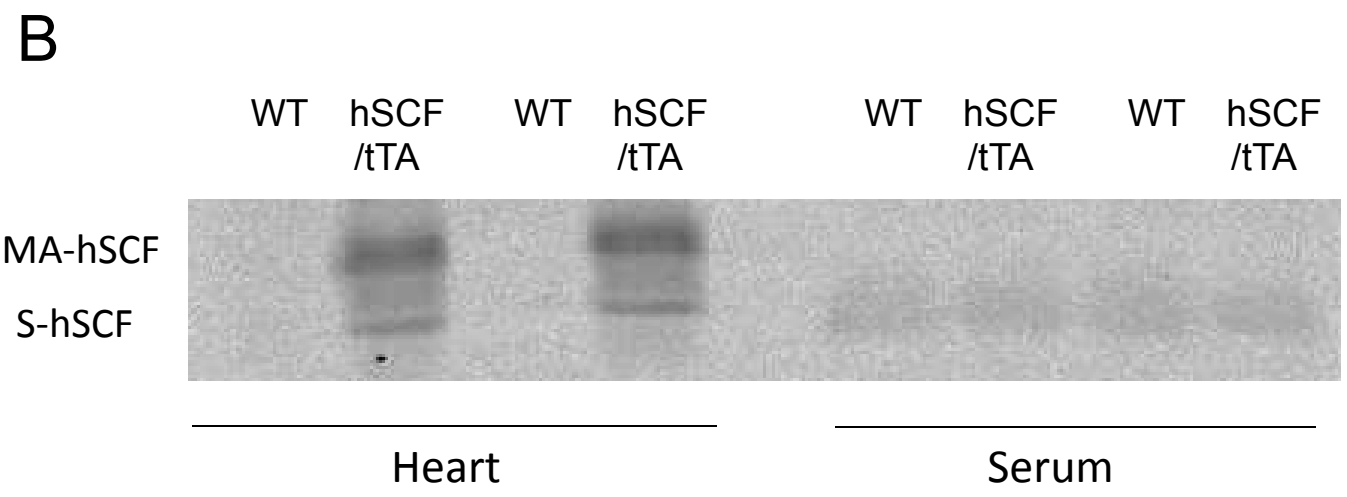
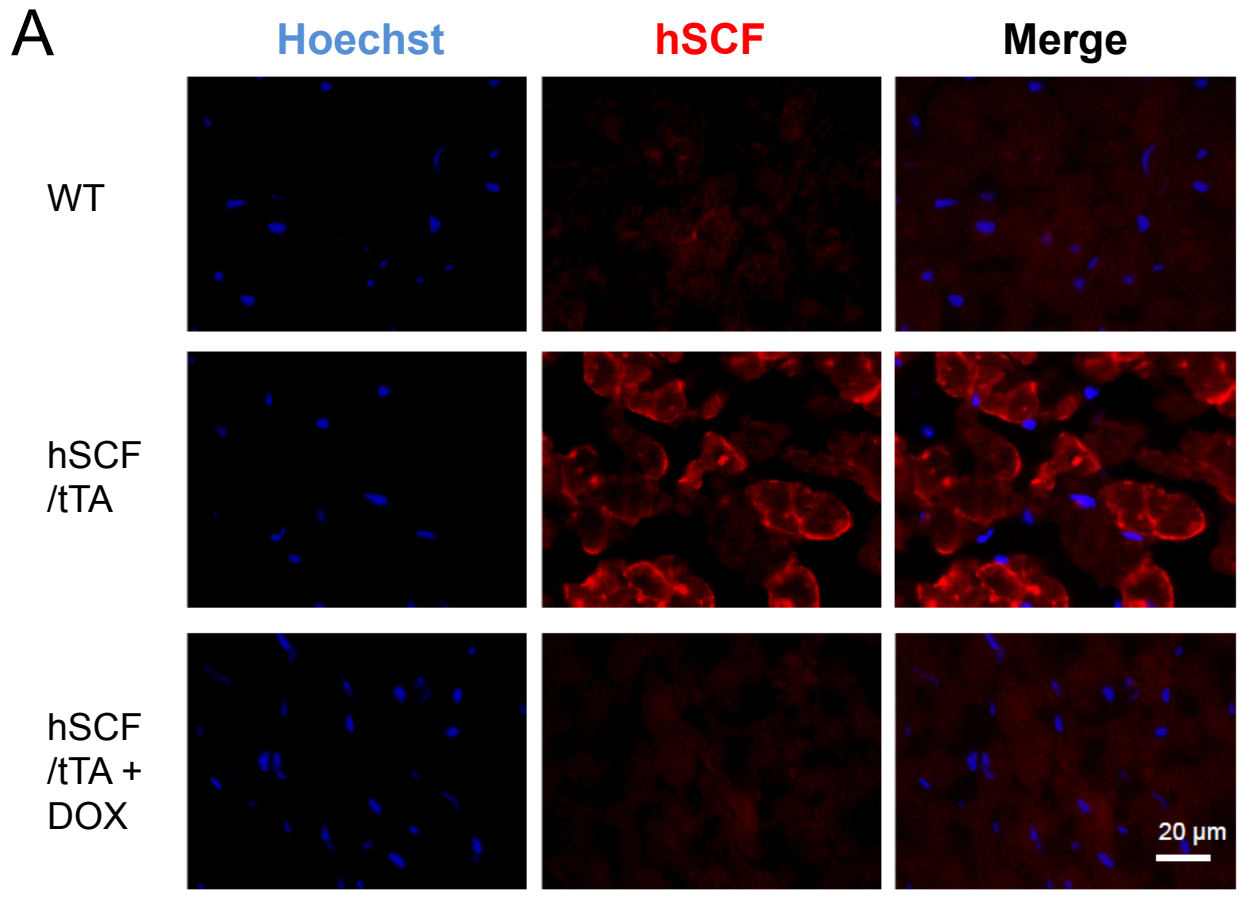
Suppl. Figure 6. Transwell EPDC migration. EGFP⁺ EPDCs were seeded on the upper inserts with 8 μ m pores. Neonatal cardiomyocytes infected with either Ad-LacZ or Ad-hSCF were seeded on the lower chamber. Cells were allowed to migrate for 24 hours in 1% fetal calf serum and the number of EGFP⁺ EPDCs migrated through the insert membrane was detected under fluorescent microscopy. Shown are representative images of EGFP⁺ EPDCs migrated through the transwell membrane.

Suppl. Figure 7: Expression of hSCF protein in adenovirus treated hearts. Heart tissues from ROSA^{mTmG};Wt1^{CreER} mice injected with Ad-hSCF or Ad-LacZ were subjected to western blot analysis. Expression of hSCF protein was observed only in Ad-hSCF treated hearts.

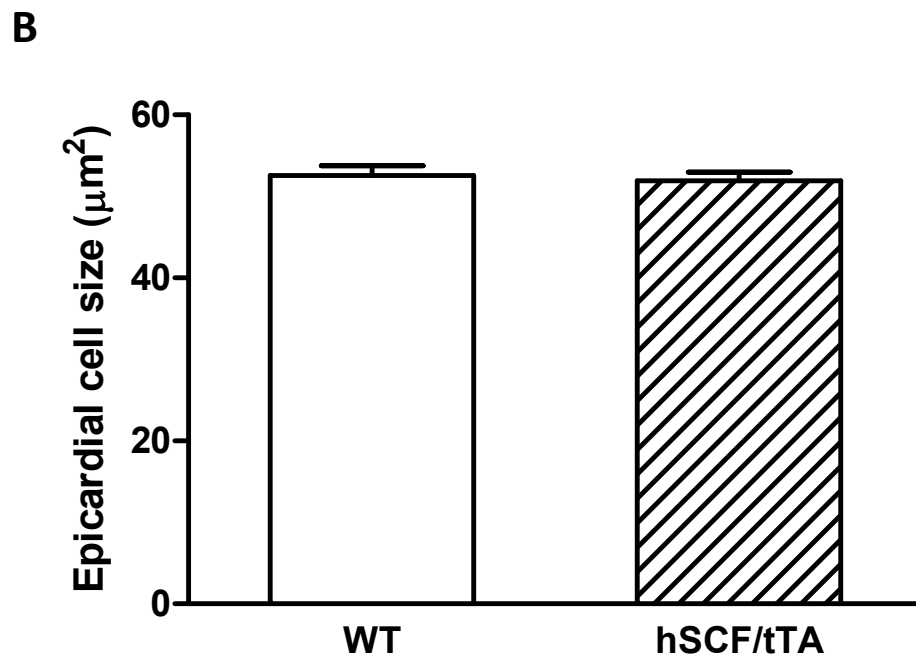
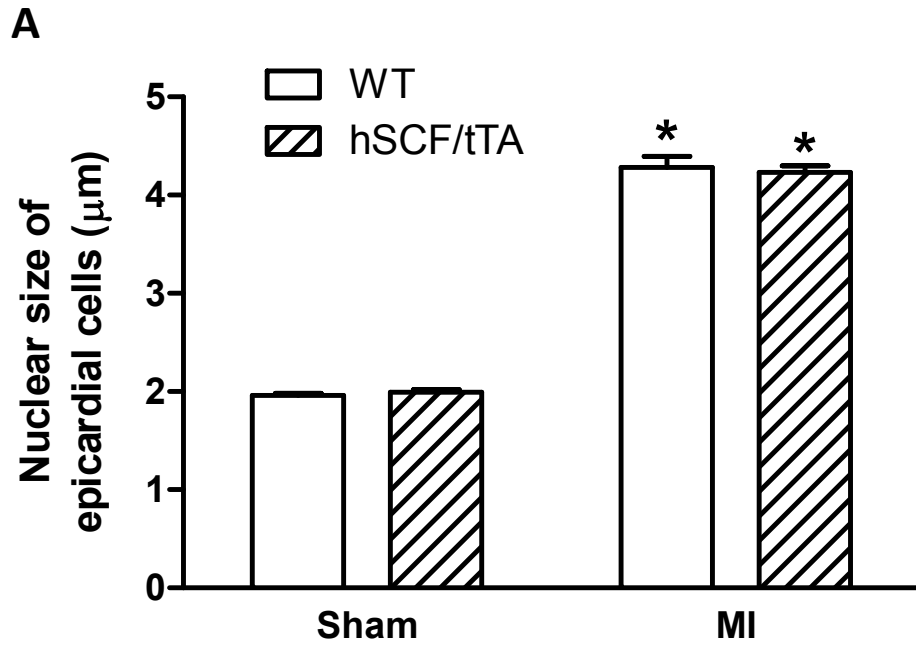
Suppl. Figure 8: *In vitro* lineage tracing of Wt1⁺ cell derived EPDCs. **A.** Representative images of EPDCs from P0 ROSA^{mTmG};Wt1^{CreER} or ROSA^{mTmG} mice treated with tamoxifen (200 nM). EGFP⁺ cells (green) were observed only in EPDCs from the ROSA^{mTmG};Wt1^{CreER} hearts. **B.** Representative images of passage 1 EPDCs from ROSA^{mTmG};Wt1^{CreER} hearts stained with EGFP and SMA (nuclei: blue, SMA: red, EGFP: green).

Suppl. Figure 9: Fate mapping of Wt1⁺ cell-derived EPDCs post-MI. **A.** Representative images of EGFP and FSP1 staining of Wt1-derived EPDCs in the infarcted myocardium. The EGFP⁺ cells are also positive for FSP1. **B.** Percent FSP1⁺/EGFP⁺ to total EGFP⁺ cells were similar between Ad-hSCF and Ad-LacZ treatment, both around 50%. Data are mean \pm SEM, n=6 per group. Unpaired student *t* test: *P*=n.s.

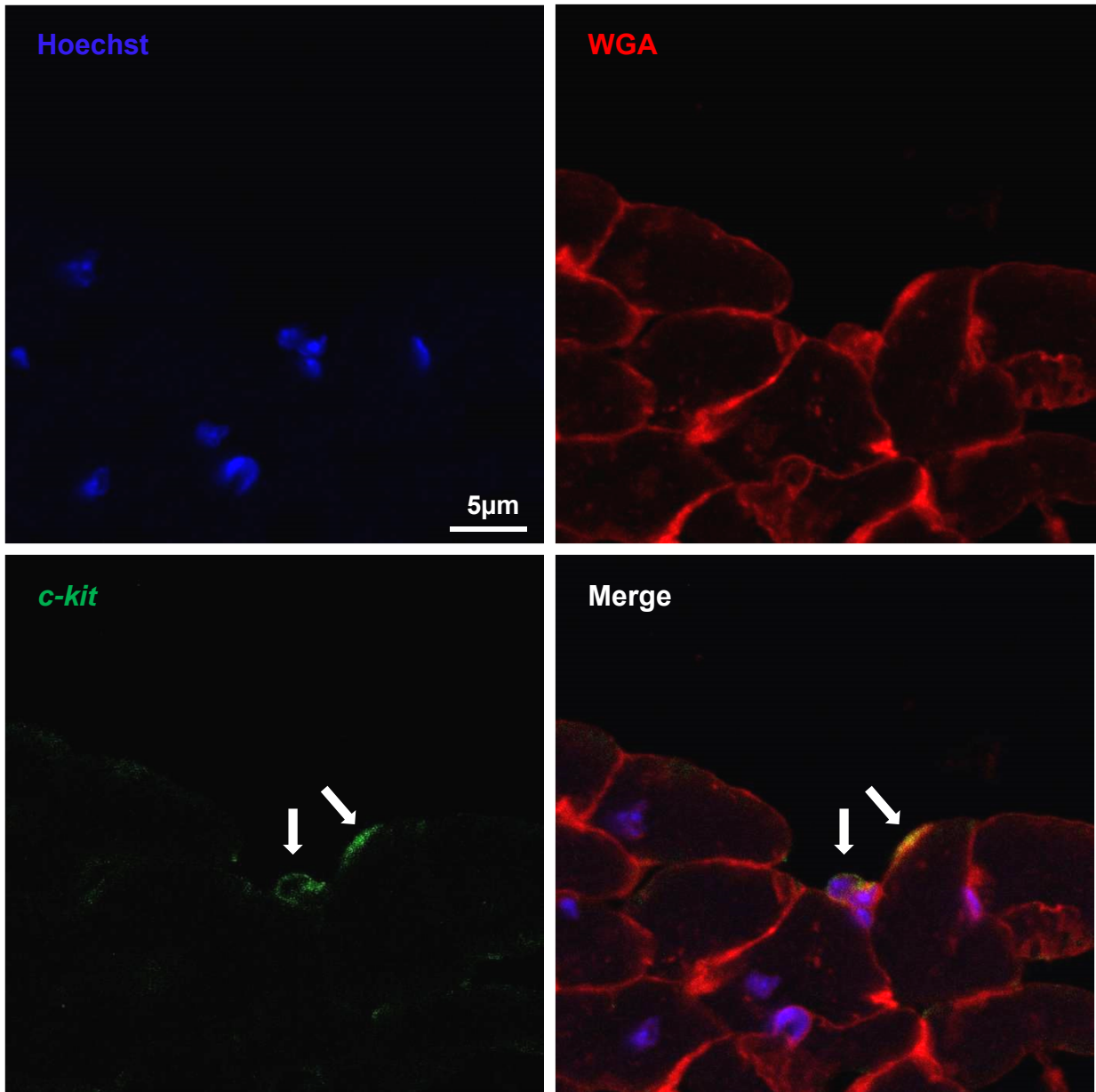
Suppl. Figure 10: Representative images of *c-kit* and TGF β R2 double staining of epicardial cells post-MI. Upper panel: A *c-kit*⁺ cell (green) is shown in the peri-infarct area of the epicardium. Lower panel: TGF β R2⁺ cells (red) are seen in the epicardium and subepicardium of the infarcted area. No *c-kit* and TGF β R2 double positive epicardial cells were found in WT or hSCF/tTA mice (n=4 per group). Nuclei, blue.



Suppl. Figure 1

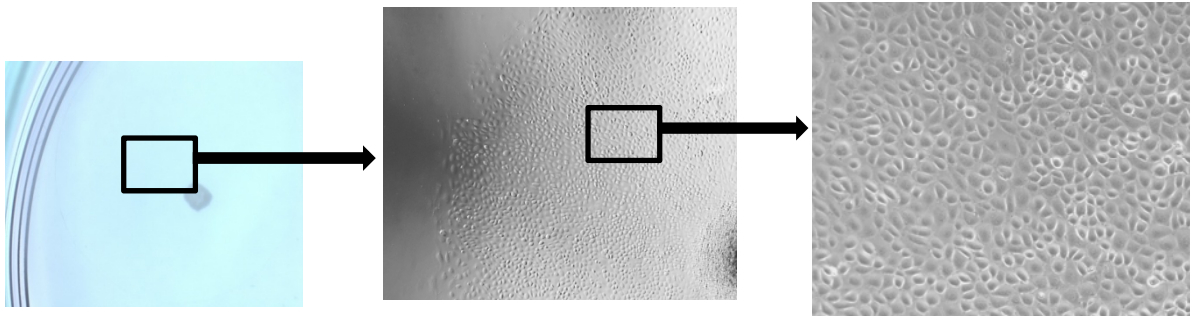


Suppl. Figure 2



Suppl. Figure 3

A

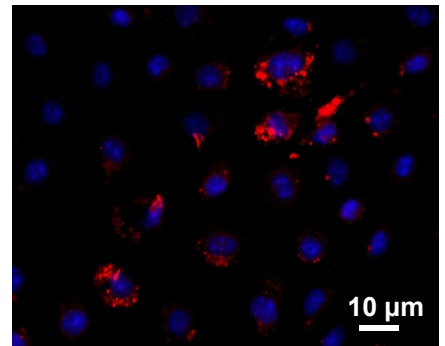
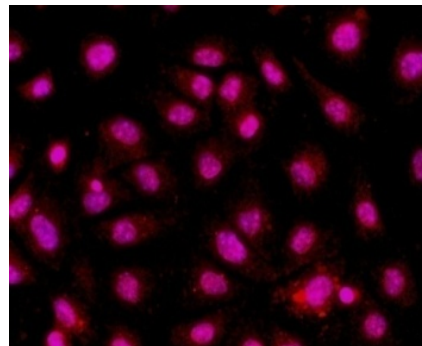
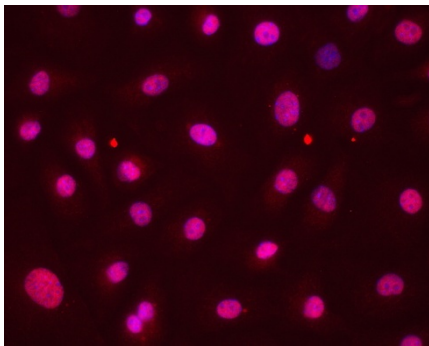


B

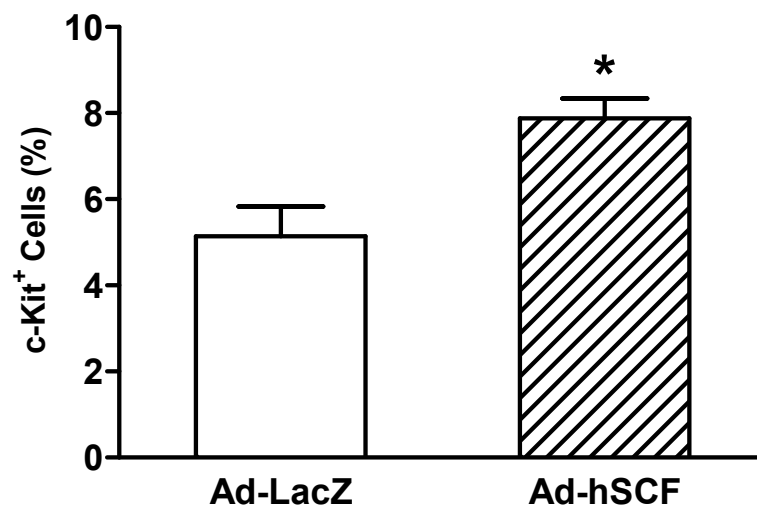
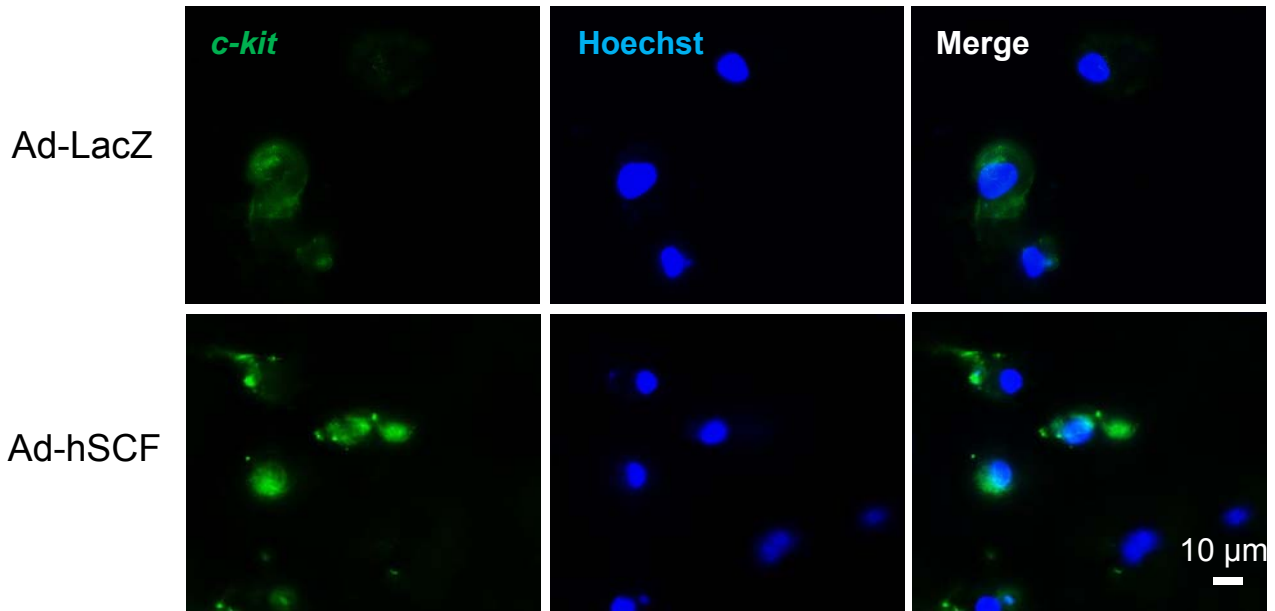
Epicardin

Wt1

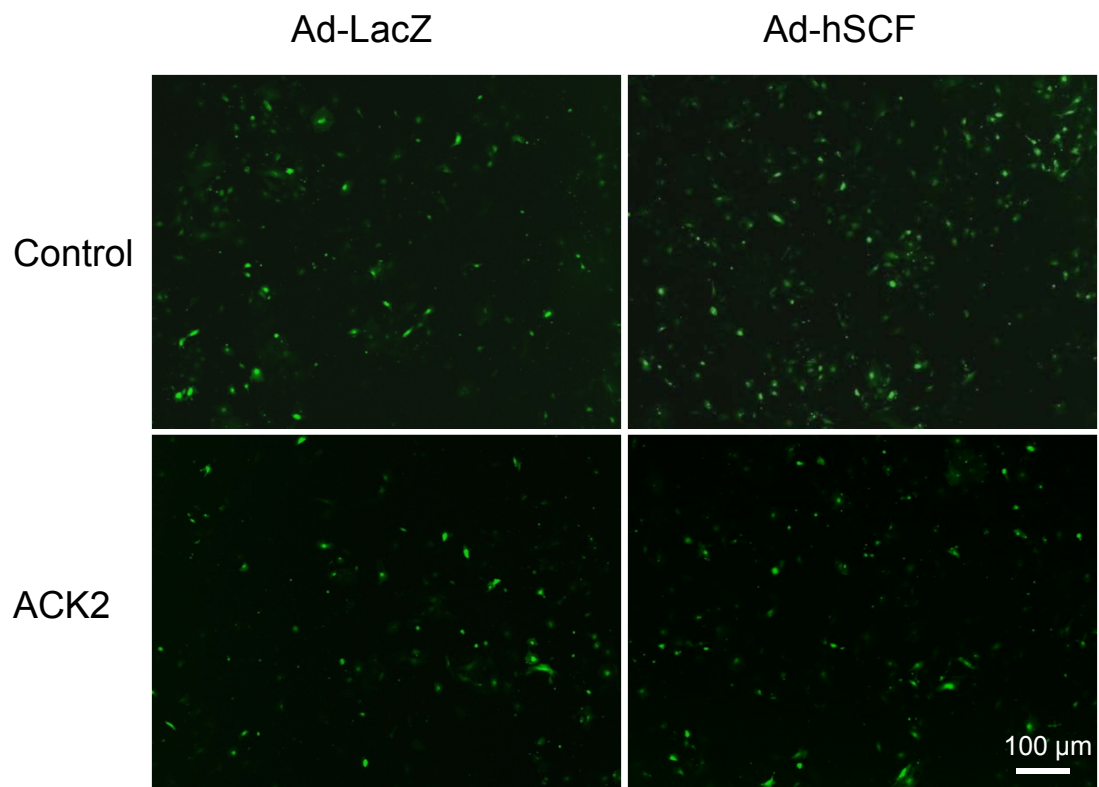
c-kit



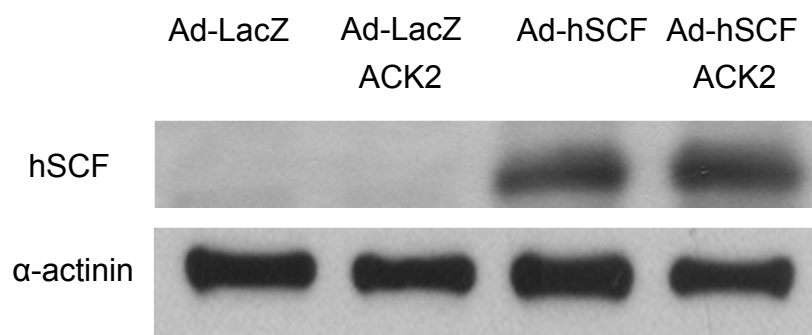
Suppl. Figure 4



Suppl. Figure 5

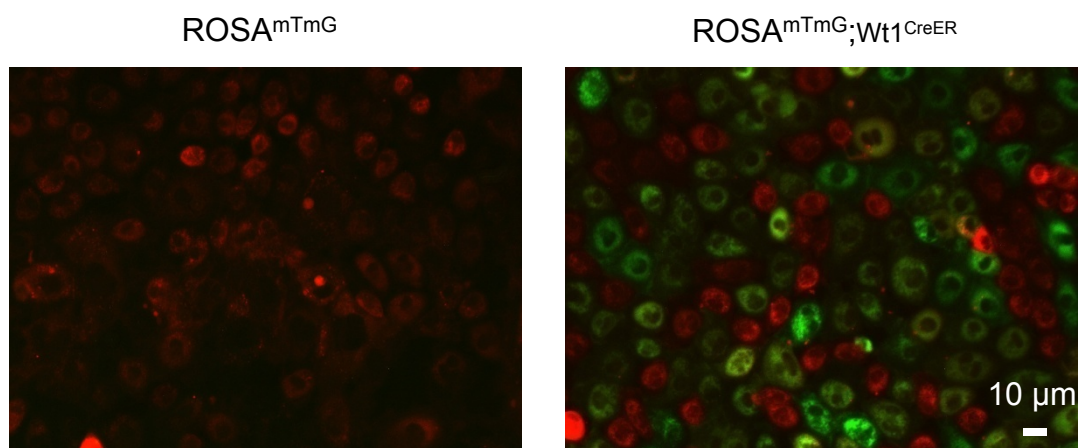


Suppl. Figure 6

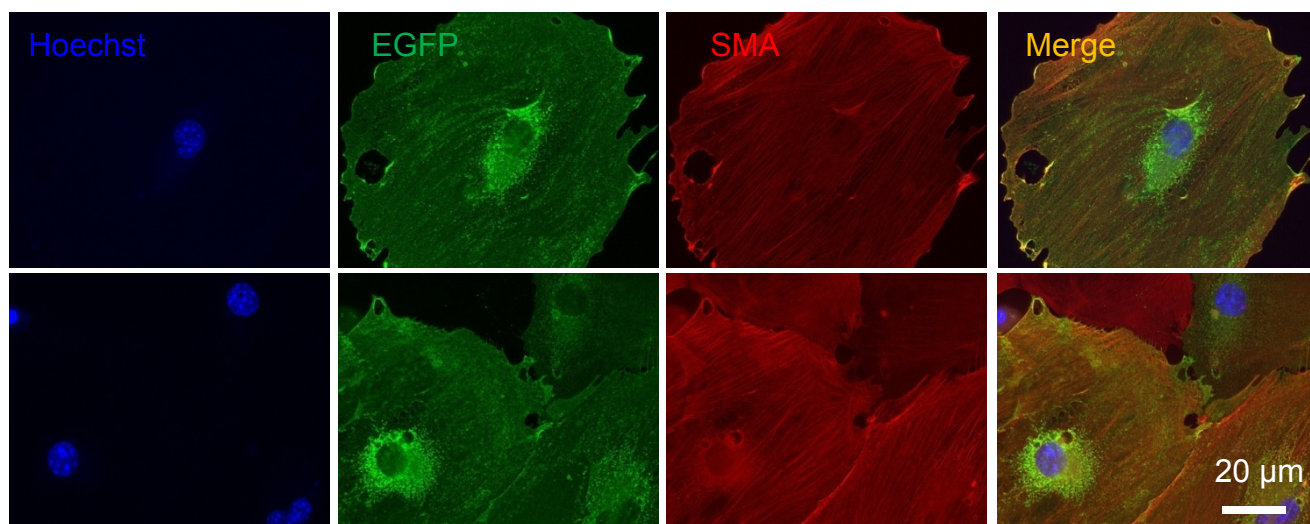


Suppl. Figure 7

A

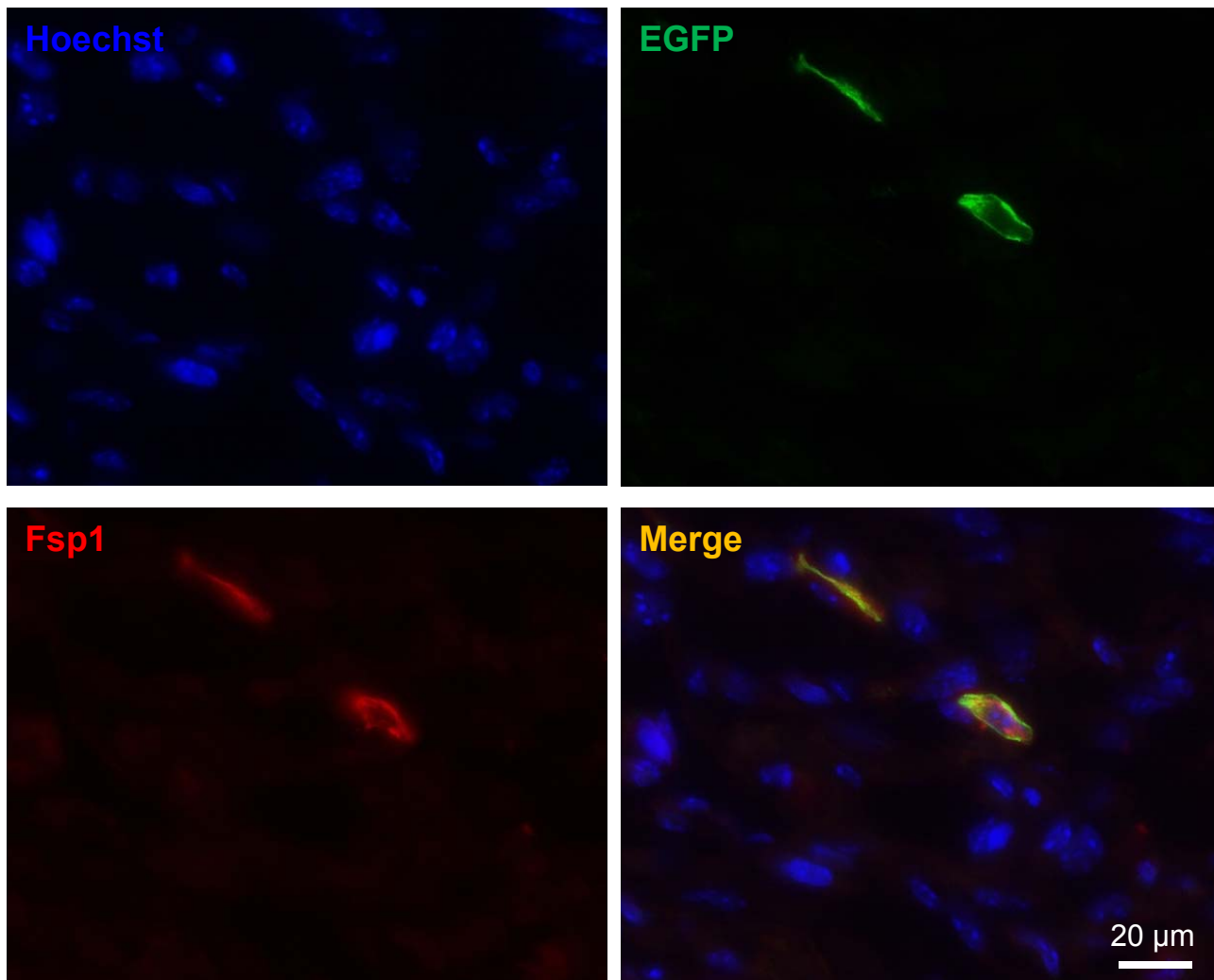


B

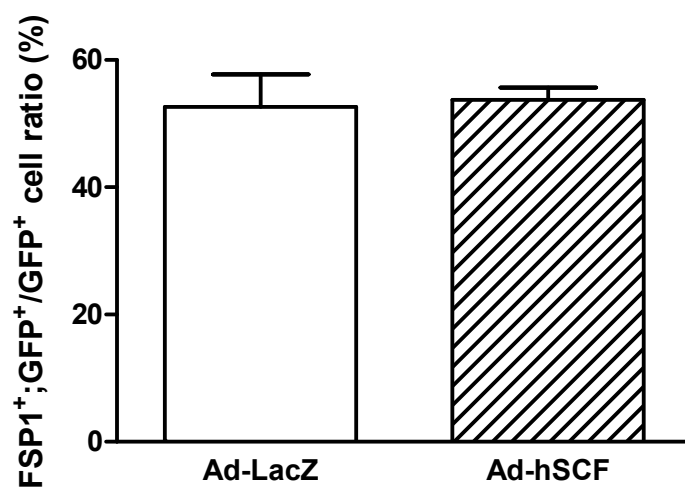


Suppl. Figure 8

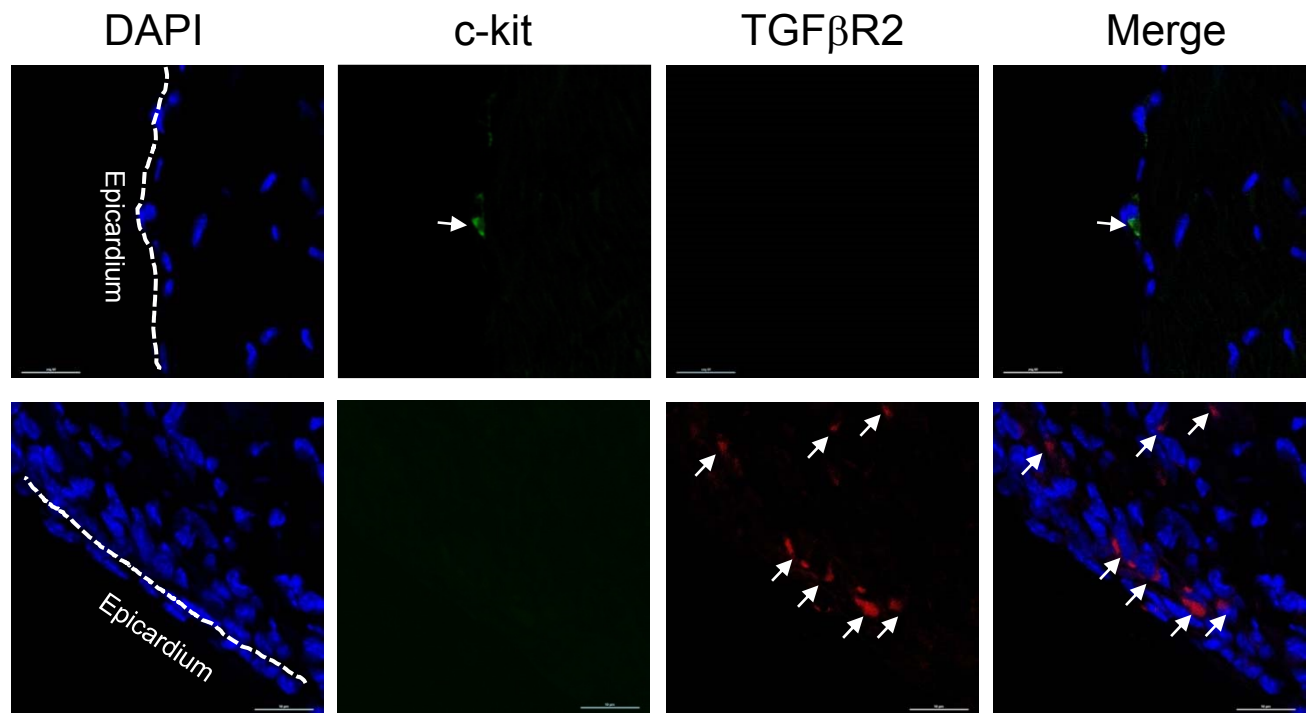
A



B



Suppl. Figure 9



Suppl. Figure 10